Sonic Superradiance in Bose Einstein Condensates

Andrew J. S. Reid

A thesis submitted for the degree of
Bachelor of Science with Honours in Physics of
The Australian National University

November, 2005

Declaration

This thesis is an account of research undertaken between February 2005 and November 2005 at The Department of Physics, Faculty of Science, The Australian National University, Canberra, Australia.

Except where acknowledged in the customary manner, the material presented in this thesis is, to the best of my knowledge, original and has not been submitted in whole or part for a degree in any university.

Andrew J. S. Reid
November, 2005

Acknowledgements

Aside from the eventual failure to actually find any results, this past year has been a highly enjoyable experience, although somewhat tense towards the end. For making it so I would like to thank Dr Craig Savage, my supervisor, for having a fairly good idea of when to prod me into action, encouraging me, and providing frank and yet heartening discussion of my future prospects and the life of a physicist. I must also thank Dr Joe Hope and Sebastian Wuester for their help with my research, and in particular with my understanding of the numerical simulation package XMDS and ideas about resolving problems with the simulations. I am also extremely grateful to my parents, for providing support from a distance through well placed comments, for shouldering the financial burden of my expenses to give me the best possible chance of succeeding, and for raising me in such a way that I became someone interested in physical research, which is possibly the most fascinating form of activity I have yet encountered. I also could not have reached the end of this year without my many friends, by whose patience with me as I gradually descending into increasing neuroticism and constantly babbled about topics only a theoretical physicist could care about I am astonished. Without their support I suspect I would have long since become stark raving mad.

Abstract

There are a number of interesting phenomena that are predicted to be a result of the behaviour of general relativity close to a black hole. The most well known of these is Hawking radiation. Although well established, the theory of Hawking radiation is unsupported by experiment, since black holes cannot be investigated in the lab. However, there is a strong similarity between the equations governing the behaviour of a sound wave in inviscid irrotational fluid systems and a massless scalar field in a gravitational system. This similarity provides hope that effects like Hawking radiation can be investigated in analogous fluid systems.

The requirement that potential fluid analogues be barotropic, inviscid and irrotational indicates that superfluids would be the logical object of experiments designed to analyse such systems. The most easily controlled superfluid to which experimentalists have access is a Bose Einstein Condensate in an appropriately designed trap, and there is interest in designing an experiment to look for Hawking radiation in a BEC. A BEC is also ideal for that purpose because of the extremely low temperatures at which the condensation occurs, given the very low temperature of Hawking radiation. However, Hawking radiation itself is a very subtle effect, and it would be very hard to detect.

This means that a related but more conspicuous effect is interesting as a stepping stone to a test for the more well known Hawking radiation. This related effect is Superradiance, a result of the reflection of an incoming scalar field with appropriate angular characteristics from the ergoregion of a massive rotating body such as a black hole. An ergoregion is a region around a rotating black hole or supermassive rotating star within which it is impossible to remain stationary with respect to an observer at infinity without exceeding the speed of light.

Before an experiment can be designed to test for superradiance in a BEC it is necessary to establish whether the theory describing Bose-Einstein Condensates predicts that it will actually occur. Work on this problem thus far has either failed to consider whether the effect occurs, and instead focused on the consequences it would have, or has involved approximations that are not strictly valid. Here therefore, after an overview of both the analogy between fluid and gravitational systems and the specific theory related to Bose Einstein Condensates is an analysis using the full quantum theory of BECs.

The initial consideration is analytic in character, but the equations do not allow for an exact solution within the approximations attempted that predict superradiance, so a change is made to a numerical simulation using the XMDS numerical simulation package. Unfortunately, this attempt also fails, since ongoing problems encountered in running the simulation consumed all the time available. A discussion of these problems is included.

Contents

List of Figures

Chapter 1

Introduction

The Theory of General Relativity conceived by Einstein has made a number of predictions that are startlingly accurate. However, it has also made a number of surprising predictions that cannot be checked experimentally, and are unlikely to be observed through the various forms of telescope developed by astrophysicists. In particular, the predictions regarding "black holes", regions of spacetime from which even light cannot escape [1] are unlikely to ever have direct experimental verification. Regions of space suspected of being black holes can be observed, but there are finer detail predictions made regarding the interaction of the boundaries of these regions of space with the area around them that these observations cannot help with. In particular, in 1974 Hawking [2] predicted that the interaction of quantum mechanics with the boundary of the region from which light cannot escape, the "event horizon", would lead to a gradual radiation of energy by the black hole, with a thermal spectrum. This phenomena is extremely interesting, but there is no experimental investigation possible.

It has also been predicted that a rotating black hole or supermassive star will have an ergoregion, within which staying stationary with respect to an observer at infinity would require traveling faster than the speed of light due to the dragging of spacetime around the object. The interactions of scalar fields with an ergoregion have been shown to imply that a scalar field with the right characteristics approaching the black hole or star could be reflected from the ergoregion with greater amplitude, an effect called superradiance [1, 3, 4].

These predictions are interesting, but seemed destined to be inaccessible for verification until 1981, when Unruh proposed a possible analogy between scalar fields in gravitational systems and sound waves in flowing inviscid irrotational fluids [5], that is, fluids that flow without viscosity and for which the curl of the fluid flow is 0. Unruh demonstrated that the derivation of Hawking radiation could be performed in such a fluid system, and work by others indicated that a number of gravitational systems could be so duplicated.

This analogy held the promise of allowing a test of Hawking radiation. Unfortunately, the temperature of the radiation predicted in a fluid system was far too low to be measured in any system available at the time. In the last ten year, however, rapid advancement in the technology of cooling gases has allowed the creation of Bose-Einstein Condensates, dilute gas systems in which every atom occupies a single quantum state [6, 7, 8, 9, 10]. These systems have a very simple quantum description, and also exist at temperatures measured in nanokelvin. Since in certain conditions they can to a degree be described as inviscid and irrotational fluids, these BECs are of extreme interest to researchers seeking to perform an experiment to test Hawking radiation.

However, Hawking radiation is a subtle effect, and so it would be of great assistance to begin by investigating a related, but much stronger, effect. Superradiance is just such a phenomena. Since it is a magnification of an incident scalar field in astrophysics, or an incident sound wave in a fluid system, the size of the effect is under experimental control. Therefore, it would be much easier to detect, which makes it a very attractive first step on the road towards verifying Hawking radiation. Superradiance is also interesting in its own right, and verification of its validity would be worthwhile regardless of the connection to Hawking radiation.

Before any experiment attempting to demonstrate superradiance can be begun it is necessary to investigate whether it will in fact occur in a BEC, and under what conditions it is to be expected. In the literature at present there is no definitive answer to this question. There is some strong evidence provided by the work of Slatyer and Savage [11], but their work made use of an approximation, called the hydrodynamic approximation, that is of dubious merit. They investigated a system in which a vortex in a BEC was used to create the analogue ergoregion, and the approximation is that the density of the gas at no point changes too quickly. However, in the core of a BEC vortex the density of the condensate does drop rapidly, and it is in this region that the physics leading to superradiance occurs. The results of the work are therefore suspect, and further investigation without this approximation is necessary before any definitive answer can be given.

This then forms the question behind this thesis, does the effect that serves as the analogy to astrophysical superradiance, the reflection of sound waves with greater amplitude from a BEC vortex, actually occur?

After an overview of the concepts from general relativity, the fluid analogy, and the theory of Bose-Einstein condensates is provided a review of the previous work on this question, and a discussion of the limitations on it is made. Following this, the original work that formed my honours project will be presented. This consisted firstly in an attempt to find an analytic solution to the equations of motion of the system that would predict superradiance. However, this first direction failed, as no sufficiently general solution could be found, and the narrow solution that was achieved did not predict that superradiance was possible. As a result of this failure, an attempt was made to numerically simulate a reflection of a wavepacket from a vortex. This work, however, was hampered by unusual and unexpected results from the numerical simulation indicating an unknown flaw in the simulation, that could not be identified and resolved before the time available for the honours project was exhausted. As such, unfortunately, the question remains open.

1.1 Thesis Plan

In Chapter 2 an overview of the concepts from general relativity involved in superradiance is presented, particularly the definitions of ergoregions and superradiance, as well as an account of the analogy between fluid systems and gravitational systems. A derivation indicating that the analogy is genuine and a discussion of the limitations on it are presented.

A description of Bose-Einstein Condensates is presented in Chapter 3. A discussion of the advantages of a BEC as an analogue gravity system is made, and the microscopic theory of the condensate is derived, along with the semiclassical approximations that lead to the derivation of analogue gravity. The hydrodynamic approximation and the consequences of making it are also covered.

The focus of Chapter 4 is on the work of Slatyer and Savage [11], which provides the most immediate precursor to the original work that follows. In particular, the derivation of an analytic condition for superradiance is reproduced, and the numerical results presented in that paper are also duplicated. A discussion then follows of the limitations on that work that are a consequence of the hydrodynamic approximation.

Chapter 5 is primarily a return to the microscopic theory of BECs, although a response to a possible objection to geometries where a vortex is at the centre of a uniform condensate producing superradiance is discussed. The objection is that in such a geometry the condensate is in a state of zero energy, and as such there is no way to extract energy through superradiance. The response is that although not always interpreted in that way the equations used to describe perturbations on the condensate can be considered to represent occupation of uncondensed quasiparticle modes in the condensate, which can have negative energy. The chapter also contains a derivation of the Bogoliubov deGennes equations in preparation for the following chapter.

It is in Chapter 6 that the original work begins, this chapter contains the derivation of an analytic solution of the BdG equations under certain approximations that do not include the hydrodynamic approximation. The solution that is derived is very highly constrained in the behaviour in the angular direction of the cylindrically symmetric system considered, and also predicts that superradiance will not occur within those constraints. However, the solution was promising, in that it took a form remarkably similar to that found by Slatyer and Savage [11], although not reproducing their exact outcome.

This is not a satisfactory response, since it lacks the generality necessary to rule superradiance out as well as not predicting it, and as such a numerical simulation was sought. Chapter 7 contains a description of the choices made regarding what form of the equations of motion to use, what form to use for the background, how the initial state should be defined, and why these choices were made.

Following this, Chapter 8 contains a description of the outcome of these simulations, which alas were not definitive. A number of problems with the script could not be located and resolved before the time available to an honours project ended, and so regrettably no response to the principle question can be presented. Some discussion of the difficulties faced and images of the flawed results obtained are given.

Finally a summary of the work presented is provided, and some discussion of possible ways to resolve the still unanswered principle question is made, as well as mention of other related areas of research.

Chapter 2

The Fluid Analogue and Superradiance

2.1 The Hydrodynamic Analogy

It was first noted by Unruh [5] that the equations that describe the propagation of a massless minimally coupled scalar field in a (3+1)-dimensional spacetime can under the right conditions be the same as those that describe acoustic fluctuations of the velocity potential in barotropic, inviscid, irrotational fluids, and the analogy was further extended by Visser [12, 13]. If the fluid is described by the continuity equation, the zero-viscosity Euler equation, and has a barotropic equation of state, then it can be shown that the acoustic fluctuations will be governed by the same equation that governs the propagation of massless scalar fields in relativity, namely the Klein-Gordon equation,

$$\frac{1}{\sqrt{-g}}\partial_\mu \left(g^{\mu\nu}\sqrt{-g}\partial_\nu\phi\right) = 0. \tag{2.1}$$

In the hydrodynamic case the spacetime metric $g_{\mu\nu}$ is replaced by an effective metric which is a function of the velocity and density of the fluid serving as the background on which the acoustic fluctuations propagate.

This dual meaning for the Klein-Gordon equation suggests that appropriately constrained fluid flows can serve as effective metrics that mirror those of general relativity. In principle, this would then allow the investigation of the behaviour of quantum and classical fields in various metrics by investigating the behaviour of sound waves in fluid systems. While there are constraints and flaws involved in the analogy, it does offer the possibility of investigating systems and phenomena that, being rooted in general relativity, cannot be observed or created in a laboratory setting.

2.1.1 Derivation of the Klein-Gordon Equation in a Fluid

In order to demonstrate the analogy with relativistic systems the derivation from the equations of the fluid system to the Klein-Gordon equation will be shown here. However, when actually investigating fluid systems it is seldom necessary to actually use the Klein-Gordon equation, and bypassing it can lead to a simpler calculational route. This means that this derivation serves as a proof of the concept used in what follows, rather than a basis for the calculations. In the tensor equations presented here and throughout this work the presence of one raised and one lowered index indicates implicit summation over that index (the Einstein summation convention)

The starting point for the derivation is an irrotational and barotropic fluid that is non-relativistic. Irrotational in this case means that the velocity field of the fluid is curl free, and barotropic means that the local pressure is a function solely of the local density. It can be demonstrated that requiring barotropicity ensures that an initially irrotational flow will remain so over time [12], which thus implies that the flow will remain curl free. Because of this, it possible to define a scalar potential θ in such a way that $\vec{v} = \nabla\theta$.

As mentioned above, the equations from which the derivation begins are the continuity equation 2.2, the zero-viscosity Euler equation 2.3, and a barotropic equation of state, presented below. Of course, using equation 2.3 as an equation of motion of the system requires that the fluid is viscosity free.

$$\frac{\partial \rho}{\partial t} + \nabla \cdot (\rho \vec{v}) = 0, \tag{2.2}$$

$$\rho \left(\frac{\partial \vec{v}}{\partial t} + (\vec{v} \cdot \nabla)\, \vec{v} \right) = -\nabla p, \tag{2.3}$$

$$p = p(\rho). \tag{2.4}$$

Where ρ is the density field of the solution.

By selecting some exact background solution to the system of equations the bulk motion of the fluid is selected, and then small fluctuations around that bulk motion are considered. These fluctuations are denoted $(\hat{\rho}, \hat{p}, \hat{\theta})$, and the speed of sound is defined as c, where $c^2 = \partial p / \partial \rho$, and the equations of motion for the fluctuations are therefore

$$\frac{\partial \hat{\rho}}{\partial t} + \nabla \cdot \left(\hat{\rho} \nabla \theta + \rho \nabla \hat{\theta} \right) = 0, \tag{2.5}$$

$$\rho \left(\frac{\partial \hat{\theta}}{\partial t} + \nabla \theta \cdot \nabla \hat{\theta} \right) = \hat{p}, \tag{2.6}$$

$$\hat{p} = c^2 \hat{\rho}. \tag{2.7}$$

Combining these differential equations results in a single second order differential equation for the perturbation,

$$\frac{\partial}{\partial t} \left(\frac{\rho}{c^2} \left(\frac{\partial \hat{\theta}}{\partial t} + \vec{v} \cdot \hat{\theta} \right) \right) = \nabla \cdot \left(\rho \nabla \hat{\theta} - \frac{\rho \vec{v}}{c^2} \left(\frac{\partial \hat{\theta}}{\partial t} + \vec{v} \cdot \hat{\theta} \right) \right). \tag{2.8}$$

To make the analogy plain, it is possible to define four dimensional coordinates such that,

$$(t, x, y, z) \rightarrow (x_0, x_1, x_2, x_3). \tag{2.9}$$

With this transformation the single differential equation 2.8 can be reexpressed in the form

$$\frac{1}{\sqrt{-g}} \partial_\mu (g^{\mu\nu} \sqrt{-g} \partial_\nu \hat{\theta}) = 0, \tag{2.10}$$

and $g^{\mu\nu}$ is here representing the inverse effective metric, which is written as

$$g^{\mu\nu} = \frac{1}{\rho c} \left(\begin{array}{c|c} -1 & -v_j \\ \hline -v_i & (c^2 \delta_{ij} - v_i v_j) \end{array} \right) \tag{2.11}$$

with i and j taking values $\{1, 2, 3\}$ as is conventional, and $g = [det(g^{\mu\nu})]^{-1}$.

This is the Klein-Gordon equation describing the behaviour of a minimally coupled scalar field propagating in a spacetime with the inverse metric $g^{\mu\nu}$, thus demonstrating the theoretical foundation for the gravitational analogy to fluids satisfying the conditions mentioned at the beginning of this section.

2.1.2 The Effective Metric

For a cartesian coordinate system the metric, inverse metric, and metric determinant are given by

$$g_{\mu\nu} = \frac{\rho}{c}\left(\begin{array}{c|c} -(c^2 - v^2) & -v_j \\ \hline -v_i & \delta_{ij} \end{array}\right), \tag{2.12}$$

$$g^{\mu\nu} = \frac{1}{\rho c}\left(\begin{array}{c|c} -1 & -v_j \\ \hline -v_i & (c^2\delta_{ij} - v_i v_j) \end{array}\right), \tag{2.13}$$

$$g = -\frac{\rho^4}{c^2}. \tag{2.14}$$

It is also of use to know the effective metric for cylindrical polar coordinates, since these are sometimes more convenient. Indeed, in the case of a fluid vortex, which is the systems discussed later as a possible system in which to investigate superradiance, cylindrical polar coordinates are much more intuitively appropriate. For cylindrical coordinates the four-dimensional coordinates are related to the polar coordinates by

$$(t, r, \theta, z) \rightarrow (x_0, x_1, x_2, x_3). \tag{2.15}$$

The metric, inverse metric, and determinant are given by

$$g_{\mu\nu} = \frac{\rho}{c}\begin{pmatrix} -(c^2 - v^2) & -v_r & -rv_\theta & -v_z \\ -v_r & 1 & 0 & 0 \\ -rv_\theta & 0 & r^2 & 0 \\ -r_z & 0 & 0 & 1 \end{pmatrix}, \tag{2.16}$$

$$g^{\mu\nu} = \frac{1}{\rho c}\begin{pmatrix} -1 & -v_r & -\frac{v_\theta}{r} & -v_z \\ -v_r & c^2 - v_r^2 & -\frac{v_r v_\theta}{r} & -v_r v_z \\ -\frac{v_\theta}{r} & -\frac{v_r v_\theta}{r} & \frac{c^2 - v_\theta^2}{r^2} & -v_r v_z \\ -v_z & -v_r v_z & -v_r v_z & c^2 - v_z^2 \end{pmatrix}, \tag{2.17}$$

$$g = -\frac{\rho^4}{c^2} r^2. \tag{2.18}$$

2.1.3 Possible Problems with the Analogy

Assumptions On Which the Derivation Relies

In order for the calculations given above to be accurate a number of assumptions about the fluid and perturbation field have been made. The density and velocity have been assumed to be representable by continuous classical fields, which requires that the length scales of the system are long enough to ignore the microscopic structure of the fluid. This means behaviour with small length scales is not covered by the analogy, which is unfortunate as the small length scale behaviour of astrophysical systems is not itself known. As such, the dependence of long length scale effects on small length scale structure is of interest, and investigation of such problems in hydrodynamic systems where the microscopic structure is well enough understood to not make investigating it prohibitively difficult may provide insight on possible solutions in the astrophysical cases, although the relation between the two systems in such cases is not guaranteed [14, 15, 16, 17].

Another assumption that was made explicit in the derivation is that the fluid is irrotational, inviscid, and barotropic. If these conditions are not met the derivation is clearly suspect, although how great the impact would be isn't immediately apparent. In the case of a fluid that is to some degree rotational, the definition of the velocity field $\vec{v}$ is impossible, which is highly problematic, since it is this field which forms the analogue of the scalar field, without which the exercise is somewhat moot. Failure of the barotropic condition is equally dire, since it will lead to a failure of the irrotational condition over time, as previously mentioned [12]. Possibly less problematic is the presence of viscosity, and such systems have been investigated by Visser [13] and Schutzhold and Unruh [18].

The analogy is also dependent on the fluctuations being small, since the derivation has been performed on the basis that there is no significant back reaction by the perturbation on the fluid background. In addition, the analogy does not extend to the behaviour of the metric, so any changes in the effective metric introduced by the perturbation would render the evolution of the system of dubious merit as an analogy. Therefore, any process that leads to rapid growth of the fluctuation field will quickly cease to be covered by the perturbative derivation and the analogy.

In addition, it is not necessarily the case that the zero-viscosity Euler equation applies completely to the system being investigated. In particular, Bose-Einstein Condensates, although inviscid, only approximately obey the zero-viscosity Euler equation. The full equation contains an additional term that results in complications to the theory unless it can be ignored, which provides a restriction on the parameter regimes within which this analogy is valid. More detail on this topic will be provided when the specific equations governing BECs are discussed in section 3.3.

Mechanics of the Background

As mentioned briefly above, it is important to remain aware of the limit of the analogy to a mapping between the behaviour of sound waves in a fixed background fluid flow and the behaviour of scalar fields in a fixed background spacetime. There is no link between the behaviour of the fluid background and the behaviour of the spacetime background. This is clear because the effective metric for the hydrodynamic system is calculated from the background density and phase, the evolution of which are governed by the continuity and zero-viscosity Euler equations, whereas the astrophysical metric evolves in a fashion governed by the Einstein field equations, which would be expected to result in very different evolutions if the backgrounds are not held fixed. This can be expressed as an analogy for kinematic properties of the system only, dynamical properties are not preserved [12]. Again as mentioned above, any back reaction from the fluctuations on the background that are taken into account will result in changes that cannot be mapped between the two different regimes. This to some extent limits the behaviour that can be investigated via the analogy. For example, black hole entropy is an intrinsically dynamical effect [12] which will not occur in a hydrodynamic system.

This limitation also implies that it is in general impossible to exactly duplicate a solution of the Einstein equations with an effective metric. As an example, there is no choice of velocity and density profiles that will give rise to an analogue of the Schwarzschild metric describing an uncharged spherically symmetric black hole [12]. However, it is possible to identify the important features of an astrophysical system, such as the presence of an event horizon in the case of the Schwarzschild black hole, and create effective metrics that mirror these features, rather than the metric as a whole, and it is in this way that the analogy is applied.

Limitations on Quantum Effects

Many of the effects that would be most interesting to duplicate via the hydrodynamic analogy are intrinsically quantum in nature, one of the most well known of these being Hawking radiation. However, Unruh and Schutzhold [19] have demonstrated that it is not sufficient to reproduce the Klein-Gordon equation with an effective metric if it is a quantum effect that is sought. After examining a "slow light" system designed as an optical black hole analogue in great detail they conclude that while the system reproduces classical effects such as the presence of an event horizon and mode mixing at that horizon, it does not give rise to analogue Hawking radiation due to the behaviour of the commutation relations for the relevant field in that system.

The crucial difference is that while the mode mixing, which is a classical phenomenon, is preserved, this does not necessarily equate to particle production in the outgoing modes. The quantum commutation relations link the Bogoliubov modes to the notion of particles, and the particle production which is associated with Hawking radiation is dependent on the commutation relations allowing a physically reasonable interpretation where the various modes have excitations which can be viewed as particles.

However, in the cases of Bose-Einstein Condensates and non-dispersive linear dielectric media Unruh and Schutzhold demonstrate that the commutation relations are, within the regimes where the approximations required for the analogy are valid, equivalent to those for a quantum scalar field in the corresponding curved space-time. This provides a substantial advantage to these systems as areas of investigation, and to Bose-Einstein Condensates in particular, which are relatively easy to manipulate. It is this preservation of quantum properties that provides the strongest motivation for the investigation in BECs that follows.

2.2 Ergoregions and Superradiance

The motivation for investigating the hydrodynamic analogy is provided by a curiosity regarding implications of the theory behind astrophysical phenomena like black holes and ultrarelativistic rotating stars. Predictions regarding these systems are novel, unlikely to be directly observable, and impossible to test directly in a lab [5, 20, 13, 21, 22, 23]. The original proposal Unruh made [5] was specifically about so-called "dumb holes", the hydrodynamic analogue of black holes, so named because they do not permit sound to escape. Unruh's results have been extended and generalised [12, 13, 24], and other authors have considered other systems, such as rotating black holes, or "white holes" [12, 21, 25, 26]. In each of these systems there are certain characteristics of the system that are considered crucial, and these are duplicated by the fluid flows.

The most essential feature of a black hole is the event horizon. This is a boundary of a region in space-time where the trajectories of all particles that are moving forward in time (referred to as "timelike geodesics") point inward, away from the boundary. Because of this, there is no future time at which a particle, having crossed the boundary, will be found outside it.

There is another noteworthy area that surrounds a black hole, referred to as an ergoregion. An ergoregion is the region within which a particle may not remain stationary relative to an observer far from the black hole, since that would require exceeding the speed of light. The boundary of an ergoregion is called the ergosphere. For a stationary black hole the ergosphere corresponds to the event horizon, and in that case the ergoregion has little extra effect. However, a rotating black hole, or a rapidly rotating and very dense star will drag the reference frame of nearby observers around in the direction of rotation, an effect called frame dragging. This will in the case of a black hole extend the ergoregion, moving the ergosphere outside the event horizon, and in the case of the rotating star can create a region where remaining stationary requires motion exceeding the speed of light, even though there is no point where moving directly away requires it.

One of the most discussed reasons to investigate analogue gravitational systems is the investigation of Hawking radiation, which is the spontaneous emission of thermal radiation from a black hole, a consequence of the behaviour of quantum fields in a metric containing an event horizon first proposed by Hawking in 1974 [2]. There is however another effect that is a consequence of the presence of the ergoregion, called superradiance.

Superradiance, in the context of astrophysics, is the name given to an effect whereby wavepackets incident on an ergoregion may under the right conditions be reflected with increased amplitude [1, 3, 4]. The amplified reflection in general only occurs for wavepackets below a certain frequency. Superradiance, unlike Hawking radiation, is a classical effect that can be derived directly from the equations of motion for a classical scalar field in a curved spacetime. Because of the classical nature of superradiance there is no need to quantise fields when investigating it, which simplifies attempts to determine whether an analogue system will manifest it. In addition, the stimulated nature of the effect means that in a laboratory setting it would be much easier to observe than the weak Hawking radiation effect. As such, it warrants investigation as a potential stepping stone to investigating Hawking radiation, in addition to curiosity regarding superradiance itself.

2.2.1 Acoustic Superradiance

The fluid analogue of a black hole event horizon is the sonic horizon, a surface at which the velocity of the fluid perpendicular to the surface is equal in magnitude to the speed of sound [12, 13]. Moving away from an analogue black hole horizon, the perpendicular flow velocity increases in the direction of flow, and thus inside a black hole horizon the speed of sound is less than the flow velocity directly away from the horizon, so even sound waves that are aimed directly at the horizon cannot propagate back towards it, since that would require their propagation speed to be faster than the local speed of sound.

An analogue ergoregion is unsurprisingly that region in the fluid where the magnitude of the flow velocity is greater than the local speed of sound, and the ergosphere is the surface where the flow velocity is equal to the local speed of sound. It follows from this that an event horizon must always be either contained within or coincide with an ergosphere, since there cannot be a surface from which the perpendicular velocity has equal magnitude to the speed of sound without the overall magnitude of the flow speed being equal to or greater than the speed of sound.

In systems that are either one dimensional or effectively one dimensional, the ergosphere and the event horizon must coincide. This is also the case for systems with certain symmetries, for example if the flow velocity variation in a cylindrically or spherically symmetric system is purely radial. However, there are also flow velocity profiles where the ergosphere is found outside the event horizon. One possible example of this is a cylindrically symmetric draining vortex [12], where the horizon will be found where the radial flow has greater magnitude than the speed of sound, whereas the ergosphere will be located where the total magnitude of the flow, in both the radial and angular directions, is equal to the speed of sound. This sort of draining vortex could serve as an analogy for a black hole, and would be a possible configuration in which to investigate acoustic superradiance [21]. The analogue of superradiance itself is an increase in the reflected amplitude of a sound wave incident on an acoustic ergoregion, which should in principle be easy to detect.

However, there is another, simpler, system that can be used. It is also possible to create an analogue ergoregion with a vortex that does not drain. In this case, the ergosphere will be found when the angular flow has greater magnitude than the speed of sound, since there is no radially directed motion. This system is more closely analogous to a dense rotating star, and has been investigated by Slatyer and Savage [11]. By removing the need for draining and replenishing the fluid being used, such a system would be easier to create experimentally, especially in the case of Bose-Einstein Condensates, which are highly fragile and thus difficult to replenish in a continuous fashion. It is this sort of system that will be discussed throughout this work, and the results Slatyer and Savage derived will be discussed in chapter 4, since they serve as the immediate precursor to the original work in chapters 6, 7, and 8.

Chapter 3

Theory of Bose-Einstein Condensates

3.1 Bose-Einstein Condensation

A Bose-Einstein Condensate is a gas of indistinguishable bosons at sufficient density that has been cooled to low enough temperatures for the single particle ground state to be macroscopically occupied. This is only possible for bosons, particles with integer spin, since only bosons will share the same quantum state. Although the theory of this effect was developed some time ago by Bose [27] and Einstein [28] in 1924-25, it was only demonstrated in 1995 [8, 9, 10] after significant advances in cooling techniques made it possible to reach the necessary temperatures with sufficient densities.

Historically BECs have been most easily created with dilute gases of alkali atoms cooled to nanokelvin temperatures, most often in a magnetic, optical, or combined magnetic and optical trap that is approximately harmonic in each direction. Rubidium [8], lithium [9], and cesium [10] have all been used in experiments. With the alkali atom gases the interaction between the atoms can be approximated via a contact potential, since at the temperatures involved only the s-wave scattering interaction occurs. The system is also well suited to a mean field description due to the macroscopic occupation of the single particle ground state and the low densities involved.

3.2 Advantages of BECs as Gravitational Analogues

When the gravitational analogy to fluids was first discussed it was mentioned that one of the primary motivations for the study of such systems is the possibility to study effects that cannot be observed in gravitational systems, such as Hawking radiation. Hawking radiation itself is a quantum effect that has a very low temperature, and therefore BECs, with their relatively simple quantum description and very low background temperature, would be ideal for attempting to reproduce it. Superradiance, conversely, is classical in nature, so a BEC isn't immediately apparent as a the best system with which to investigate it. A BEC is difficult to produce in a lab, and there may be more simply achievable systems to use, such as the water based model considered by Schutzhold and Unruh [18]. However, these systems would be forced to contend with viscosity, turbulence, and environmental effects that would significantly complicate the process. BECs, being both superfluid when in an appropriate trap and by necessity very well isolated from external effects, can mostly ignore these issues.

As will be shown in the derivations to follow, the condensed fraction of a BEC will evolve in a fashion very similar to that of a zero viscosity irrotational classical fluid as discussed in section 2.1. However, the fluid equations contain an extra higher order derivative term, which would substantially complicate any calculation. This term, referred to as the quantum pressure term because of its units, is proportional to a characteristic length in the condensate governed by several parameters of the system. It is common to ignore this term when investigating gravity analogues, in what is known as the hydrodynamic approximation, however the validity of doing so in the investigation of superradiance is dubious, as will be discussed later.

It is possible to derive equations for the effective metric in the BEC case, and thus arrive at the same equations as in section 2.1, when applying the hydrodynamic approximation, or a similar equation where the effective metric is no longer comprised of functions, but rather differential operators, when the higher order derivative term is retained, as shown by Visser [20]. For some cases this method may be preferable, however in this case it is the equation of motion for a perturbation in the condensate that is important. This means that working with the form of the equations that directly mirrors that of general relativity is largely superfluous once analogous behaviour has been established as resulting from the equations from which one begins, as in section 2.1.1. Therefore, derivation of the equation of motion for the perturbation from the equations governing a condensate will be via a more direct route here.

3.3 Microscopic Theory of BECs

3.3.1 The Gross-Pitaevskii Equation

If the Bose field operator for the condensate is $\hat{\Psi}$, then in the mean field approximation the classical field is defined as $\psi\left(\vec{r},t\right) = \langle\hat{\Psi}\left(\vec{r},t\right)\rangle$ where $\langle\hat{\Psi}\left(\vec{r},t\right)\rangle$ is used to denote the expectation value of the operator, as is usual in quantum field theory, and a fluctuation $\hat{\Psi}'\left(\vec{r},t\right)$ is defined by

$$\hat{\Psi}\left(\vec{r},t\right) = \psi\left(\vec{r},t\right) + \hat{\Psi}'\left(\vec{r},t\right) \tag{3.1}$$

When this fluctuation is small compared to the classical field equations of motion for both parts of $\hat{\Psi}$ can be derived by expanding the equation of motion for the Bose field operator to lowest orders in the perturbation, effectively producing two equations.

The Hamiltonian for the BEC system is a combination of the single particle Hamiltonian and an inter-particle interaction term, which can be written as

$$\hat{H} = \int \mathrm{d}\vec{r}\hat{\Psi}^{\dagger}\left(\vec{r}\,\right) H^{sp}\hat{\Psi}\left(\vec{r}\,\right) + \frac{1}{2}\int \mathrm{d}\vec{r}\mathrm{d}\vec{r}\,'\hat{\Psi}^{\dagger}\left(\vec{r}\,\right)\hat{\Psi}^{\dagger}\left(\vec{r}\,'\right)V\left(\vec{r}-\vec{r}\,'\right)\hat{\Psi}^{\dagger}\left(\vec{r}\,',t\right)\hat{\Psi}^{\dagger}\left(\vec{r},t\right). \tag{3.2}$$

Using the usual single particle Hamiltonian, the commutation relations for the boson field operator, and the Heisenburg equation of motion, this results in the equation for the time evolution of the field operator,

$$\begin{aligned} i\hbar\frac{\partial}{\partial t}\hat{\Psi}\left(\vec{r},t\right) &= [\hat{\Psi},\hat{H}] \\ &= \left(-\frac{\hbar^2\nabla^2}{2m} + V_{\mathrm{trap}} + \int \mathrm{d}\vec{r}\,'\hat{\Psi}^{\dagger}\left(\vec{r}\,'\right)V\left(\vec{r}-\vec{r}\,'\right)\hat{\Psi}\left(\vec{r}\,',t\right)\right)\hat{\Psi}\left(\vec{r},t\right). \end{aligned} \tag{3.3}$$

As previously mentioned, at these temperatures the interaction term can be approximated by the s-wave scattering, which can be represented by an effective contact potential parametrised by the s-wave scattering length a, giving

$$V\left(\vec{r}-\vec{r}\,'\right)=U_0\delta\left(\vec{r}-\vec{r}\,'\right), \tag{3.4}$$

$$U_0=\frac{4\pi\hbar^2 a}{m}. \tag{3.5}$$

Substituting this into the equation of motion, and taking the expectation value of the field operator results in the mean field equation of motion,

$$i\hbar\frac{\partial}{\partial t}\psi\left(\vec{r},t\right)=\left(-\frac{\hbar^2\nabla^2}{2m}+V_{\text{trap}}+U_0|\psi\left(\vec{r},t\right)|^2\right)\psi\left(\vec{r},t\right). \tag{3.6}$$

This widely applicable equation is the Gross-Pitaevskii equation, and describes the motion of a classical field corresponding to the condensate, providing the back reaction from the perturbation is not too great.

3.3.2 Hydrodynamic Equations in a BEC

The Gross-Pitaevskii equation is a description of the evolution of a condensate with negligible or no fluctuation, and it can also be expressed in a form that makes the fluid character of the condensate explicit. If the mean field ψ is expressed as

$$\psi=\sqrt{\rho}\,e^{i\theta} \tag{3.7}$$

with ρ a real positive function and θ a real function, then the derivatives of ψ in terms of the new variables are

$$\nabla\psi=\nabla\left(\sqrt{\rho}\,e^{i\theta}\right)=i\psi\nabla\theta+\psi\frac{\nabla\rho}{2\rho}, \tag{3.8}$$

$$\nabla^2\psi=\nabla\psi\cdot\left(i\nabla\theta+\frac{\nabla\rho}{2\rho}\right)+\psi\left(i\nabla^2\theta+\frac{\nabla^2\rho}{2\rho}-\frac{|\nabla\rho|^2}{2\rho}\right), \tag{3.9}$$

$$\frac{\partial\psi}{\partial t}=i\frac{\partial\theta}{\partial t}\psi+\frac{\psi}{2\rho}\frac{\partial\rho}{\partial t} \tag{3.10}$$

which can be substituted into the Gross-Pitaevskii Equation (3.6), the result of which is

$$i\hbar\left(i\frac{\partial\theta}{\partial t}+\frac{1}{2\rho}\frac{\partial\rho}{\partial t}\right)=-\frac{\hbar^2}{2m}\left(\left(i\nabla\theta+\frac{\nabla\rho}{2\rho}\right)^2+\left(i\nabla^2\theta+\frac{\nabla^2\rho}{2\rho}-\frac{|\nabla\rho|^2}{2\rho^2}\right)\right)+V+U_0\rho. \tag{3.11}$$

When split into real and imaginary parts the equation is divided into a pair of equations in ρ and θ,

$$-\hbar\frac{\partial\theta}{\partial t}=-\frac{\hbar^2}{2m}\left(-|\nabla\theta|^2-\frac{|\nabla\rho|^2}{4\rho^2}+\frac{\nabla^2\rho}{2\rho}\right)+V+U_0\rho, \tag{3.12}$$

$$\frac{\hbar}{2\rho}\frac{\partial\rho}{\partial t}=-\frac{\hbar^2}{2m}\left(\frac{1}{\rho}\nabla\theta\cdot\nabla\rho+\nabla^2\theta\right). \tag{3.13}$$

These equations can be somewhat simplified by defining $\vec{v}=(\hbar/m)\nabla\theta$ [6]. Since all gradients are curl free,

$$\nabla\times\vec{v}=\frac{\hbar}{m}\nabla\times\nabla\theta=0. \tag{3.14}$$

This definition of $\vec{v}$ combined with taking the gradient of 3.12 allows the rewriting of equations 3.12 and 3.13 in terms of $\vec{v}$, which results in two new equations,

$$\frac{\partial \vec{v}}{\partial t} = \nabla\left(-\frac{1}{2}\vec{v}\cdot\vec{v} + \frac{\hbar^2}{2m^2\sqrt{\rho}}\nabla^2\sqrt{\rho} - \frac{V}{m} - \frac{U_0\rho}{m}\right), \tag{3.15}$$

$$\frac{\partial \rho}{\partial t} + \nabla\cdot(\rho\vec{v}) = 0. \tag{3.16}$$

Of these equations, 3.16 is identical to the continuity equation (2.2), and since $\nabla\times\vec{v} = 0$,

$$\nabla\left(\vec{v}\cdot\vec{v}\right) = 2\left(\vec{v}\cdot\nabla\right)\vec{v}, \tag{3.17}$$

which allows further simplification of equation 3.15, which now takes the form

$$\frac{\partial \vec{v}}{\partial t} + \left(\vec{v}\cdot\nabla\right)\vec{v} = \frac{\hbar^2}{2m^2}\nabla\left(\frac{1}{\sqrt{\rho}}\nabla^2\sqrt{\rho}\right) - \nabla\left(\frac{V+U_0\rho}{m}\right). \tag{3.18}$$

This reexpressed equation is very similar to the zero-viscosity Euler equation 2.3, except for the additional spatial derivative term involving ρ. This is the previously mentioned quantum pressure term [6], and as previously described, if it is small enough to be safely neglected, the condensate will behave like a zero viscosity fluid. The assumption that this is the case is called the hydrodynamic approximation, as previously mentioned.

The validity of this approximation is governed by the relative magnitude of the two terms on the right in Equation 3.18. For an idea of the approximate order at which they are of similar magnitude, if the spatial scale over which the number density of the condensate ρ varies is represented by l, then the pressure term $\nabla\left(U_0\rho/m\right)$ in equation 3.18 is of the order $U_0\rho/ml$, while the quantum pressure term is of order $\hbar^2/m^2l^3$[6]. This then means that in a very rough sense the hydrodynamic approximation is acceptable when the length scale of spatial variation in ρ is

$$l \gg \frac{\hbar}{\sqrt{2mU_0\rho}}. \tag{3.19}$$

The quantity in this condition is a recurring parameter in Bose Einstein condensates, and is referred to as the healing or coherence length, which will be refereed to as ξ when it comes up again. This condition implies that when a long length scale approximation can be applied to the system in question the hydrodynamic approximation is valid, and this is assumed in some of the derivations from previous work in this and the following chapter. However, in the case of a real BEC vortex the variation in ρ from 0 to the density far from the vortex is controlled by the angular momentum of the vortex, and for the stable vortex with a single quantum of angular momentum occurs over a distance of 5 times the healing length as calculated far from the vortex [6], with higher angular momentum increasing the distance over which the variation occurs. Since vortices with high angular momentum are unstable, and decay into multiple vortices with lower angular momentum, it is the rapidly varying density which is most likely to feature in real situations. This casts grave doubt on the results obtained using the hydrodynamic approximation, which motivates the original work discussed in chapters 6, 7, and 8.

3.3.3 Fluctuations in the Condensate in the Hydrodynamic Approximation

The behaviour of a perturbation of the condensate when the hydrodynamic approximation has been made mirrors that of a general fluid perturbation. This would be derived from the effective metric in section 2.1.1, and is unsurprising since the equations were shown to be the same once the approximation was made. This of course requires that the system satisfies 3.19, which is not necessarily going to be the case, as discussed at the end of the previous section. Consequently, it is of value to attempt to derive equations for the evolution of the perturbation without applying the hydrodynamic approximation.

Let the background field be indicated by ψ_0, and a perturbation on that field by $\epsilon\hat{\psi}$, where ϵ is a real and positive parameter $\ll 1$, thereby ensuring that the reaction of the perturbation on the background is small, without which a perturbative derivation would be invalid. The use of an overt parameter makes this condition on the derivation explicit. In addition, both the background ψ_0 and the total wavefunction $\psi = \psi_0 + \epsilon\hat{\psi}$ are required to satisfy the Gross-Pitaevskii Equation (3.6).

To derive equations that are hydrodynamic in form the wavefunctions must be expressed in terms of phase and condensate number density. ρ_0 and θ_0 will be used for the density and phase of the background, and the perturbed phase and density will be written as $\rho = \rho_0 + \epsilon\hat{\rho}$ and $\theta = \theta_0 + \epsilon\hat{\theta}$. This implies that

$$\psi_0 = \sqrt{\rho_0}e^{i\theta_0}, \tag{3.20}$$

$$\psi = \sqrt{\rho}e^{i\theta}. \tag{3.21}$$

From the two differing expressions for ψ it is possible to derive an expression for the perturbation $\hat{\psi}$ by comparing terms of first order in ϵ.

$$\begin{aligned}
\psi_0 + \epsilon\hat{\psi} &= \sqrt{\rho_0 + \epsilon\hat{\rho}}\,e^{i\left(\theta_0+\epsilon\hat{\theta}\right)} && (3.22)\\
&= \left(\sqrt{\rho_0} + \epsilon\frac{\hat{\rho}}{2\sqrt{\rho_0}}\right)e^{i\theta_0}\left(1 + \epsilon i\hat{\theta}\right) + O\left(\epsilon^2\right) && (3.23)\\
&= \sqrt{\rho_0}e^{i\theta_0} + \epsilon e^{i\theta_0}\left(\frac{\hat{\rho}}{2\sqrt{\rho_0}} + i\hat{\theta}\sqrt{\rho_0}\right) + O\left(\epsilon^2\right) && (3.24)
\end{aligned}$$

$$\hat{\psi} = e^{i\theta_0}\left(\frac{\hat{\rho}}{2\sqrt{\rho_0}} + i\hat{\theta}\sqrt{\rho_0}\right) = \psi_0\left(\frac{\hat{\rho}}{2\rho_0} + i\hat{\theta}\right). \tag{3.25}$$

The equations of motion can now be derived by substituting $\psi = \psi_0 + \epsilon\hat{\psi}$ into the Gross-Pitaevskii equation 3.6, which gives

$$\begin{aligned}
i\hbar\frac{\partial\psi_0}{\partial t} + \epsilon i\hbar\frac{\partial\hat{\psi}}{\partial t} &= \left(-\frac{\hbar^2\nabla^2}{2m} + V\right)\psi_0 + \epsilon\left(-\frac{\hbar^2\nabla^2}{2m} + V\right)\hat{\psi} && (3.26)\\
&\quad + U_0\left(|\psi_0|^2 + \epsilon\left(\psi_0\hat{\psi}^* + \psi_0^*\hat{\psi}\right) + O\left(\epsilon^2\right)\right)\left(\psi_0 + \epsilon\hat{\psi}\right). && (3.27)
\end{aligned}$$

Comparing terms of zero and first order in ϵ yields an equation of motion for the background and for the perturbation,

$$i\hbar\frac{\partial\psi_0}{\partial t} = \left(-\frac{\hbar^2\nabla^2}{2m} + V\right)\psi_0 + U_0|\psi_0|^2\psi_0, \tag{3.28}$$

$$i\hbar\frac{\partial\hat{\psi}}{\partial t} = \left(-\frac{\hbar^2\nabla^2}{2m}+V\right)\hat{\psi}+U_0\left(\psi_0\hat{\psi}^*+\psi_0^*\hat{\psi}\right)\psi_0+U_0|\psi_0|^2\hat{\psi}. \tag{3.29}$$

As we required at the beginning of the section the equation for the background is the Gross-Pitaevskii equation, so that condition has been met. Using Equations 3.20 and 3.25 to substitute for ψ_0 and $\hat{\psi}$ with the density and phase in equation 3.29 results in equations of motion for the density and phase perturbations,

$$\begin{aligned} i\hbar\Bigg(\left(\frac{\hat{\rho}}{2\rho_0}+i\hat{\theta}\right)\frac{\partial\rho_0}{\partial t} &= -\frac{\hbar^2\nabla^2}{2m}\Bigg(\psi_0\nabla^2\left(\frac{\hat{\rho}}{2\rho_0}+i\hat{\theta}\right)+\left(\frac{\hat{\rho}}{2\rho_0}+i\hat{\theta}\right)\nabla^2\psi_0 \\ +\psi_0\frac{\partial}{\partial t}\left(\frac{\hat{\rho}}{2\rho_0}+i\hat{\theta}\right)\Bigg) &\qquad +2\nabla\left(\frac{\hat{\rho}}{2\rho_0}+i\hat{\theta}\right)\cdot\nabla\psi_0\Bigg)+V\psi_0\left(\frac{\hat{\rho}}{2\rho_0}+i\hat{\theta}\right) \\ &\qquad +U_0|\psi_0|^2\psi_0\left(2\left(\frac{\hat{\rho}}{2\rho_0}+i\hat{\theta}\right)+\left(\frac{\hat{\rho}}{2\rho_0}-i\hat{\theta}\right)\right). \end{aligned} \tag{3.30}$$

Included within this equation are a number of terms that combine to give Equation 3.28 multiplied by $\hat{\psi}/\psi_0$, which can therefore be eliminated. Doing so, using $|\psi_0|^2=\rho_0$ and dividing what remains by ψ_0 results in the more tractable equation:

$$i\hbar\frac{\partial}{\partial t}\left(\frac{\hat{\rho}}{2\rho_0}+i\hat{\theta}\right)=-\frac{\hbar^2}{2m}\left[\nabla^2\left(\frac{\hat{\rho}}{2\rho_0}+i\hat{\theta}\right)+2\nabla\left(\frac{\hat{\rho}}{2\rho_0}+i\hat{\theta}\right)\cdot\left(\frac{\nabla\psi_0}{\psi_0}\right)\right]+U_0\hat{\rho}. \tag{3.31}$$

The last references to ψ_0 can be removed by using Equation 3.8 to substitute for $\nabla\psi_0$,

$$\begin{aligned} i\hbar\frac{\partial}{\partial t}\left(\frac{\hat{\rho}}{2\rho_0}+i\hat{\theta}\right) &= -\frac{\hbar^2}{2m}\Bigg[\nabla^2\left(\frac{\hat{\rho}}{2\rho_0}+i\hat{\theta}\right)+2\nabla\left(\frac{\hat{\rho}}{2\rho_0}+i\hat{\theta}\right) \\ &\qquad \cdot\left(i\nabla\theta_0+\frac{\nabla\rho_0}{2\rho_0}\right)\Bigg]+U_0\hat{\rho}. \end{aligned} \tag{3.32}$$

The real and imaginary parts of this equation give separate, coupled, equations of motion for the phase and density fluctuation,

$$-\hbar\frac{\partial\hat{\theta}}{\partial t}=-\frac{\hbar^2}{m}\left[\nabla^2\left(\frac{\hat{\rho}}{4\rho_0}\right)+\nabla\left(\frac{\hat{\rho}}{2\rho_0}\right)\cdot\left(\frac{\nabla\rho_0}{2\rho_0}\right)-\nabla\hat{\theta}\cdot\nabla\theta_0\right]+U_0\hat{\rho} \tag{3.33}$$

$$\hbar\frac{\partial}{\partial t}\left(\frac{\hat{\rho}}{\rho_0}\right)=-\frac{\hbar^2}{m}\left[\nabla^2\hat{\theta}+\nabla\left(\frac{\hat{\rho}}{\rho_0}\right)\cdot\nabla\hat{\theta}+\frac{1}{\rho_0}\nabla\rho_0\cdot\nabla\hat{\theta}\right]. \tag{3.34}$$

Expanding the ρ_0 derivatives, and making use of the continuity equation (Equation 3.16) allows some additional simplification of the second of these, giving:

$$\frac{1}{\rho_0}\frac{\partial\hat{\rho}}{\partial t}+\frac{\hbar}{m}\left[\nabla^2\hat{\theta}+\frac{1}{\rho_0}\nabla\hat{\rho}\cdot\nabla\hat{\theta}+\frac{1}{\rho_0}\nabla\rho_0\cdot\nabla\hat{\theta}\right] = \frac{\hat{\rho}}{\rho_0^2}\frac{\partial\rho_0}{\partial t}+\frac{\hbar}{m}\frac{\hat{\rho}}{\rho_0^2}\nabla\rho_0\cdot\nabla\theta_0 \tag{3.35}$$

$$-\frac{\hbar}{m}\frac{\hat{\rho}}{\rho_0}\nabla^2\theta_0. \tag{3.36}$$

Using the same definition as before, $\vec{v}=(\hbar/m)\,\nabla\theta_0$, the coupled equations for the fluctuations can be reduced to

$$\frac{\partial\hat{\theta}}{\partial t}=\frac{\hbar}{4m\rho_0}\nabla\cdot\left(\rho_0\nabla\left(\frac{\hat{\rho}}{\rho_0}\right)\right)-\vec{v}\cdot\nabla\hat{\theta}-\frac{U_0}{\hbar}\hat{\rho}, \tag{3.37}$$

and

$$\frac{\partial \hat{\rho}}{\partial t} + \frac{\hbar}{m}\nabla \cdot \left(\rho_0 \nabla \hat{\theta}\right) + \nabla \cdot (\hat{\rho}\vec{v}) = 0. \tag{3.38}$$

Once again, the contribution of the quantum pressure term makes it difficult to find a solution, and in general reducing these two equations to a single one for either of the perturbation functions is difficult. However, if the second derivative term in the first equation can be neglected, which imposes the constraint of Equation 3.19, then Equation 3.37 can be used to obtain an equation for $\hat{\rho}$ in terms of the phase and background variables only, which then allows a single equation of motion for the phase fluctuations (and thus also the density fluctuations) to be constructed. Of course, this single equation of motion exists under the same constraints that were explained as dubious for the specific case of BEC superradiance at the end of the previous section, which should be kept in mind. The single equation is derived thusly:

$$\hat{\rho} = -\frac{\hbar}{U_0}\left(\frac{\partial \hat{\theta}}{\partial t} + \vec{v} \cdot \nabla \hat{\theta}\right), \tag{3.39}$$

$$\frac{\partial}{\partial t}\left(\frac{1}{U_0}\left(\frac{\partial \hat{\theta}}{\partial t} + \vec{v} \cdot \nabla \hat{\theta}\right)\right) - \frac{1}{m}\nabla \cdot \left(\rho_0 \nabla \hat{\theta}\right) + \nabla \cdot \left(\frac{1}{U_0}\left(\frac{\partial \hat{\theta}}{\partial t} + \vec{v} \cdot \nabla \hat{\theta}\right)\vec{v}\right) = 0. \tag{3.40}$$

This equation can be simplified by use of the definition of the speed of sound in a condensate, which has the convenient form [6]:

$$c = \sqrt{\frac{\rho_0 U_0}{m}} \tag{3.41}$$

Which, when substituted into Equation 3.40 results in

$$\frac{\partial}{\partial t}\left(\frac{\rho_0}{c^2}\left(\frac{\partial \hat{\theta}}{\partial t} + \vec{v} \cdot \nabla \hat{\theta}\right)\right) - \nabla \cdot \left(\rho_0 \nabla \hat{\theta}\right) + \nabla \cdot \left(\frac{\rho_0}{c^2}\left(\frac{\partial \hat{\theta}}{\partial t} + \vec{v} \cdot \nabla \hat{\theta}\right)\vec{v}\right) = 0 \tag{3.42}$$

which though elaborate is expressed in a single variable, and therefore in principle solvable.

Chapter 4

BEC Superradiance in the Hydrodynamic Approximation

4.1 Derivation of Superradiance

Having derived the equations of motion for a fluctuation in a Bose-Einstein condensate it is now possible to investigate the behaviour of a fluctuation in the specific fluid flow expected to produce superradiance. The most detailed analysis of the existence of the phenomenon in a BEC is due to Slatyer and Savage [11], and is reproduced here.

The derivation begins from the Wave Equation 2.1, which requires a specification of the effective metric. For this problem a cylindrically symmetric vortex with circumferential flow only is chosen, which means the effective metric is best expressed in cylindrical coordinates. Starting from the general cylindrical metric, Equation 2.16, circumferential flow implies $\vec{v} = v_\theta \hat{\theta}$. In order to satisfy the requirement that the flow be irrotational for the analogy, it must be the case that $v_\theta = \alpha / r$, for some constant α. This means that the density and speed of sound depend only on the radial coordinate r, that they will approach asymptotic values as $r \to \infty$, and also allows a simplification of the general inverse metric Equation 2.17 that must be inserted into the wave equation. The inverse metric is now

$$g^{\mu\nu} = -\frac{1}{\rho c} \begin{pmatrix} 1 & 0 & \frac{\alpha}{r^2} & 0 \\ 0 & -c^2 & 0 & 0 \\ \frac{\alpha}{r^2} & 0 & \frac{\alpha^2 - r^4 c^2}{r^6} & 0 \\ 0 & 0 & 0 & -c^2 \end{pmatrix}. \tag{4.1}$$

Making use of this effective metric assumes that the system obeys the zero viscosity Euler Equation 2.3 and the Continuity Equation 2.2, which in a BEC means that the hydrodynamic approximation has been made, and the constraint on the validity of derivations in this approximation given in Equation 3.19 applies.

A solution of the form of a cylindrical wave with angular wavenumber m, $\phi(t, r, \theta, z) = \psi(r, t) e^{-im\theta}$ is assumed, and this and the effective inverse metric are inserted into the wave equation. In a BEC with constant interaction strength the square of the speed of sound is proportional to the density [6], which can be used to eliminate the density from the wave equation, which results in

$$\frac{\partial^2 \psi}{\partial t^2} - 2i \frac{m\alpha}{r^2} \frac{\partial \psi}{\partial t} - \frac{1}{r} \frac{\partial}{\partial r} \left(r c^2 \frac{\partial \psi}{\partial r} \right) + \frac{m^2}{r^2} \left(c^2 - \frac{\alpha^2}{r^2} \right) \psi = 0. \tag{4.2}$$

The next step is to make another simplification using single frequency waves of the form $\psi(t, r) = r^{-1/2} G(r^*) e^{i\omega t}$, which given the cylindrical nature of the wave is expected.

In addition a "tortoise coordinate" r^* which is $dr/dr^* = \tilde{c}^2$ is defined, with $r^* \to r$ for $r \to \infty$ and $\tilde{c} = c/c_\infty$. Combining this simplified wave with the tortoise coordinate changes the equation into

$$\frac{\mathrm{d}^2 G\left(r^*\right)}{\mathrm{d}r^{*2}} + \frac{\tilde{c}^2}{c_\infty^2}\left(\omega^2 - \mathrm{V}_{eff}\right) G\left(r^*\right) = 0, \tag{4.3}$$

with an effective potential introduced to make the similarity to a time independent Schrödinger equation clear, where

$$\mathrm{V}_{eff} = \frac{2m\omega\alpha}{r^2} + \frac{m^2}{r^2}\left(c^2 - \frac{\alpha^2}{r^2}\right) - \frac{1}{2r}\left(\frac{c^2}{2r} - \frac{\mathrm{d}c^2}{\mathrm{d}r}\right). \tag{4.4}$$

A full solution to these equations is not obvious, but the cases where the tortoise coordinate approaches $\pm\infty$ it is possible to find a solution. For large r $r^* \approx r$ and all terms except those of highest order in r are negligible, leaving

$$\frac{\mathrm{d}^2 G\left(r^*\right)}{\mathrm{d}r^{*2}} + \frac{\omega^2}{c_\infty^2} G\left(r^*\right) \approx 0 \tag{4.5}$$

which has the general solution

$$G\left(r^*\right) = Ae^{i(\omega/c_\infty)r^*} + Be^{-i(\omega/c_\infty)r^*}, \tag{4.6}$$

Where A and B are the constant amplitudes the of incoming and outgoing waves.

The asymptotic solution for $r^* \to -\infty$ requires the density profile for the vortex to be specified. In order to derive an analytic result the following profile is used,

$$\rho(r) = \begin{cases} \rho_\infty \frac{[(r-r_0)/\sigma]^2}{2+[(r-r_0)/\sigma]^2}, & r > r_0 \\ 0, & r < r_0 \end{cases}, \tag{4.7}$$

which although not the exact density profile for a BEC vortex, is similar to the profile for a vortex with charge $\gg= 1$ [6], where the charge of a vortex is the number of quanta of angular momentum it has, except for the introduction of a free parameter σ, which will provide the scale length that would normally be provided by the condensate healing length. Such a vortex is unstable to decay into vortices with a charge of 1, but the authors suggest that an optical potential could be used to stabilise it [29]. It is also worth noting that the stringency of the condition on the hydrodynamic approximation, equation 3.19, is somewhat reduced with this profile, since the variation in density occurs in a length scale that is greater than the healing length [30]. It also adds two new free parameters into the equation to allow control of the behaviour of the analytic solution, σ as previously mentioned, and a radius that defines a central region of zero density r_0, which would not normally be found in a BEC vortex, but could be engineered through external potentials.

Deriving now the behaviour close to the vortex, it has been assumed that $\tilde{c}^2 = \rho/\rho_\infty$, and the tortoise coordinate is

$$r^* = \int \frac{1}{\tilde{c}^2}\mathrm{d}r = r - \frac{2\sigma^2}{r - r_0}. \tag{4.8}$$

When $r \approx r_0, r^* \approx -2\sigma^2/(r - r_0)$, and $c^2 \approx c_\infty^2(r - r_0)^2/2\sigma^2$. Making use of these approximations, and discarding terms that are not of the lowest order in $r - r_0$, the asymptotic behaviour is governed by

$$r^{*2}\frac{\mathrm{d}^2G(r^*)}{\mathrm{d}r^{*2}} + \frac{2\sigma^2\Omega^2}{c_\infty^2}G(r^*) = 0, \tag{4.9}$$

$$\Omega = \omega - m\alpha/r_0^2. \tag{4.10}$$

Conveniently, this is an Euler-type equation, which has solutions $G(r^*) = |r^*|^\delta$, where

$$\delta = \frac{1}{2} \pm \gamma, \quad \gamma \equiv \mathrm{sign}(\Omega)(1 - 8\sigma^2\Omega^2/c_\infty^2)^{1/2}. \tag{4.11}$$

The general solution that is the sum of these is thus

$$G(r^*) = |r^*|^{1/2}\left(C|r^*|^\gamma + D|r^*|^{-\gamma}\right), \tag{4.12}$$

where C and D are constants. Equation 4.11 indicates that γ is either purely real or purely imaginary, and in the case where it is imaginary the solution will be oscillatory, which can be emphasised by rewriting it in the form

$$G(r^*) = |r^*|^{1/2}\left(Ce^{\gamma \ln|r^*|} + De^{-\gamma \ln|r^*|}\right). \tag{4.13}$$

This allows the solution to again be identified as outgoing and incoming waves, with C and D providing the constant amplitudes of each, in parallel with the solution for $r \to \infty$. It is important to note that the identification of incoming and outgoing waves is by the sign of the group velocity, not the phase velocity [4], which means that the sign of Ω appearing in γ is not important for that identification.

The two asymptotic solutions can be linked by use of Abel's theorem, which states that since there is no first derivative term in the equation for $G(r^*)$, the Wronskian of the solution is constant, where the Wronskian of two linearly independent solutions to a differential equation $W = y_1y_2' - y_1'y_2$, which is a reduced form of the general definition for any number of functions. In this case the Wronskians of Equation 4.6, and if γ is imaginary of Equation 4.13, are

$$W(\infty) = \frac{2i\omega}{c_\infty}\left(|B|^2 - |A|^2\right) \tag{4.14}$$

and

$$W(-\infty) = 2\gamma\left(|C|^2 - |D|^2\right). \tag{4.15}$$

In the same fashion as Vilenkin [4], a solution to for $G(r^*)$ representing a wave originating at $r = +\infty$ can be considered, which for imaginary γ will have the asymptotic form

$$G(r^*) = \begin{cases} e^{i(\omega/c_\infty)r^*} + Re^{-i(\omega/c_\infty)r^*}, & r^* \to \infty \\ T|r^*|^{1/2}e^{-\gamma \ln|r^*|}, & r^* \to -\infty \end{cases}. \tag{4.16}$$

This allows the identification of the wave amplitudes of the general solutions as $A = 1$, $B = R$, $C = 0$, and $D = T$, which can be inserted into the Wronskians, which by Abel's theorem are equal. Therefore

$$\frac{2i\omega}{c_\infty}\left(|R|^2 - 1\right) = -2\gamma|T|^2, \tag{4.17}$$

which can be solved for the reflected amplitude

$$|R|^2 = 1 - sign(\Omega)|\gamma||T|^2 \frac{c_\infty}{\omega}. \tag{4.18}$$

This makes it plain that in the case where Ω is negative and $T \neq 0$, then $|R| > 1$. This will mean that far from the vortex the amplitude of the reflected wave will be greater than that of the incident wave, and superradiance will have occurred. To bring out the conditions under which this will occur more clearly, the requirement $\Omega < 0$ can be expanded to

$$\omega < \frac{m\alpha}{r_0^2}, \tag{4.19}$$

which implies that the angular propagation of the wave, governed by m is in the same direction as the vortex flow, governed by α, since $m\alpha$ must be positive.

The presence of two conditions for superradiance, that Ω must be negative and γ purely imaginary is in contrast with the rotating black hole [4], or the draining vortex examined by Basak and Majumdar [21]. They can be combined, however, to give a frequency independent condition for superradiance. $\omega \geq 0$, so $\Omega \geq -m\alpha/r_0^2$, and the requirement for superradiance means that $0 \geq \Omega \geq -m\alpha/r_0^2$, which means that $\Omega^2 \leq (m\alpha)^2/r_0^4$. For γ to be imaginary it must be the case that $1 < 8\sigma^2\Omega^2/c_\infty^2$, which when combined with $m\alpha > 0$ implies that the frequency independent necessary condition for superradiance in this system is

$$\sigma m\alpha > \frac{c_\infty r_0^2}{2\sqrt{2}}. \tag{4.20}$$

In the case of a vortex with a charge of l it is possible to substitute for the vortex velocity constant $\alpha = l\hbar/m_{\text{atom}}$ [6], where m_{atom} is the mass of the atoms used in the condensate, and also for c_∞ in terms of the healing length ξ, $c_\infty = \hbar/(\sqrt{2}\xi m_{\text{atom}})$. The result of this is the new condition

$$\xi > \frac{r_0^2}{4\sigma l m}. \tag{4.21}$$

In principle, this is always achievable, since $\xi = (8\pi n a)^{-1/2}$ where n is the number density of the atoms, and a is the s-wave scattering length, both of which can be experimentally controlled.

4.2 Numeric Simulation of Hydrodynamic Superradiance

In order to obtain some insight into the strength of the superradiance effect using BEC like parameters, Slatyer and Savage solved the wave equation 4.2 numerically [11], using the XMDS package [31], which is briefly described in section 7.1. They used an initial Gaussian wavepacket of the form $\psi(0, r) = A(r)$ with frequency ω_0,

$$\begin{aligned} A(r) &= e^{-(r-r_{\text{init}})^2/w^2} e^{i\omega_0 r/c_\infty}, \\ \frac{\partial\psi}{\partial t}(0, r) &= \left(i\omega_0 - 2c_\infty(r - r_{\text{init}})/w^2\right) A(r). \end{aligned} \tag{4.22}$$

A wide range of parameters will lead to superradiance, provided the conditions discussed in the previous section are met. Figure 4.1 is provided as an especially obvious example of the possible strength of the effect, where analysis of the Fourier components of the real parts of the incident and reflected wavepackets shows that the dominant Fourier power is

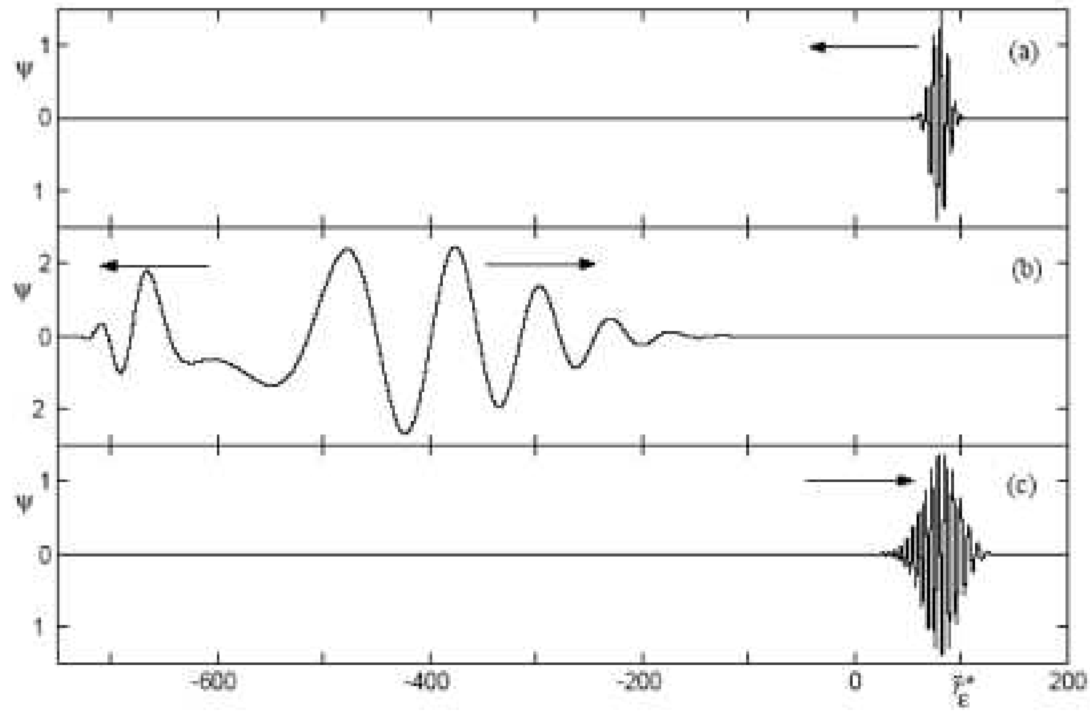

Figure 4.1: Numerical solution of wavepacket propagation in Equation 4.2. The real part of the wavepacket is plotted against a modified dimensionless radial tortoise coordinate $\tilde{r}^*_\epsilon$ described in the text. $\epsilon = 800/801$ so $\tilde{r}^*_\epsilon = -800$ at $r = r_0$. The $\tilde{t} = 0$ wavepacket is given in Equation 4.22, with $\tilde{r}_{\text{init}} = 200$ and $\tilde{w} = 10$. (a) $\tilde{t} = 114$: the wavepacket is propagating towards the vortex. (b) $\tilde{t} = 330$: the wavepacket has just been split into transmitted and reflected parts. (c) $\tilde{t} = 504$: the reflected wavepacket. The parameter values for the simulation were: $m = 1,\ \tilde{\alpha} = 2,\ \tilde{c}_\infty = 1,\ \tilde{\sigma} = 20$. There were 8192 lattice points in the spatial grid over a domain of $\tilde{r}^*_\epsilon \in [-800, 400]$. The time steps were 0.015 in the dimensionless time $\tilde{t}$.

approximately doubled. The parameters of the simulation, which are representative of a dilute trapped BEC, are given in the figure caption. The use of a tilde indicates that they have been made dimensionless by measuring distance and time in units of r_0 and ω_0^{-1}. In a Rb^{87} BEC, $m_{\text{atom}} = 1.4 \times 10^{-25} kg$, and the asymptotic healing length $\tilde{\xi} \approx 0.5$, and $\tilde{\alpha} = 2$ corresponds to a vortex charge of $l \approx 3$. In the plot, the real part of the wave is shown versus a modified radial tortoise coordinate $\tilde{r}^*_\epsilon = \tilde{r} - 2\tilde{\sigma}^2/(\tilde{r} - 1 + \epsilon)$. This magnifies the scale as $r \to r_0 (\tilde{r} \to 1)$. The ergoregion boundary for these values is at $\tilde{r} \approx 8, \tilde{r}^*_\epsilon \approx -92$.

4.3 Limitations of the Hydrodynamic Work

The principle limitation of this work is the approximation necessary to derive the single equation for the sound wave in the condensate. The elimination of the quantum pressure term described in section 3.3.3 is only acceptable when the term is small. However, the term is proportional to the healing length of the condensate

$$\xi = \frac{\hbar}{\sqrt{2mU_0\rho}}, \tag{4.23}$$

which is inversely proportional to the gas density. Unfortunately, the region in the system of most interest is precisely the region in which the density is dropping, and therefore the hydrodynamic approximation is of dubious merit. This indicates in particular that Figure 4.1(b) can not be interpreted as an actual representation of BEC behaviour. Slatyer and Savage discovered with their simulations that increasing $m, \tilde{\alpha}$, and sound wavelength increased the value of r where the maximum of their effective potential (Eqn. 4.4) was found [11]. Since they interpreted this maximum as the point of reflection, they used this to move the relevant region of their simulations away from the region where the equation they were using was invalid. This resulted in reduced, but still present, superradiance, but it remains an unsatisfactory solution to the underlying flaw in the derivation for the BEC case. The fact remains that the physics that leads to the superradiance effect occurs within the region of diminishing density. As a result, it is necessary to readdress this problem while retaining the quantum pressure term to be certain of the result, which will be considered in the chapters that follow.

Another possible concern is that the simple centrally located vortex described here represents a stable ground state solution to the equations of motion for a BEC, and it could therefore be contended that it is not possible to extract energy from the vortex, since there is no lower energy state that the vortex can move to. In fact, this is a general objection to any consideration of superradiance in such a BEC geometry, regardless of whether the hydrodynamic approximation has been made. This objection can be overcome by considering the perturbations of the condensate to represent occupation of an uncondensed quasi particle modes in the gas, which allows the possibility of negative energy modes. These negative energy modes could form the transmitted wavepacket, thus allowing for increased energy in the reflected one. The objection and response will be covered in more detail in Chapter 5.

Chapter 5

Quantum Theory of a BEC Without the Hydrodynamic Approximation

5.1 Perturbation as an Uncondensed Mode

It was mentioned at the end of Chapter 4 that a possible objection to the discussion of superradiance in that chapter was that the BEC was in a ground state of the system, and therefore no energy could be extracted. It was also noted that in any system where a uniform condensate contains a centrally located vortex will be in a ground state, and therefore vulnerable to this objection, irrespective of whether the hydrodynamic approximation has been made. Since the research to follow uses a similar background geometry, it is important to overcome this objection.

The contention is that if the background is in the ground state of the GP equation there is no lower energy state for the vortex to move to, and therefore, nowhere from which the energy amplifying the reflected wave can extracted. This would mean that superradiance is impossible. The objection is flawed, however, because it is based on the mean field approximation embodied in the Gross-Pitaevskii equation. If the sound wave being discussed were restricted to being a perturbation of the GP mean field then this objection would indeed be problematic. However the perturbation can also be considered to represent quasi-particle modes that are not part of the BEC itself [32]. These modes are fully quantum, have not been constrained to a mean field, and therefore can have negative energy. Negative energy uncondensed modes, called “anomalous modes” [33], could form the transmitted wave, which would then allow the reflected wave to have a greater energy than the incident wave by an amount equal to the magnitude of the negative energy transmitted mode. This change in interpretation also overcomes the need to consider the system as being in a superposition between the vortex and perturbation states.

From a mathematical perspective this change in interpretation is as simple as choosing an operator form of the perturbation and re-deriving the equations. The nature of the derivation is such that this does not make a significant difference to the steps followed, as can be seen in a recent review paper on analogue gravity where the derivation of the acoustic metric is performed treating the fluctuation in operator form [34].

5.2 Choice of Equations for Investigation Retaining the Quantum Pressure Term

In order to resolve the problem of the dubious validity of the results dependent on the hydrodynamic approximation, also discussed at the end of Chapter 4, it is necessary to investigate the system without making that approximation. In the first instance it is worth considering the problem analytically. The first step in such an investigation is to pick which of the several possible equations of motion will be solved. One possible choice would be to return to the point in the derivation in Section 3.3.3 where the quantum pressure term was excluded and attempt a parallel derivation retaining it. This, however, seems unreasonably difficult, since it would result in an attempt to solve a system of partial differential equations containing a number of very complicated derivative terms.

An alternative approach is to return to the Gross Pitaevskii equation and follow a different route to the derivation. A convenient alternative for analysing the behaviour of perturbations of a BEC are the Bogoliubov deGennes (BdG) equations. These equations are derived from the Gross-Pitaevskii equation to describe the behaviour of small amplitude oscillations around the background solution describing the bulk motion of the condensate [7]. These equations are simpler because they avoid the chain derivative terms found in the equations in the hydrodynamic form, Equations 3.37 and 3.38. They also have the advantage that it is more straightforward to see the way in which the derivation supports the interpretation of the perturbation as an uncondensed mode of the condensate as discussed in Section 5.1.

The starting point of the derivation of the BdG equations is the Gross-Pitaevskii equation as derived in Section 3.3.1,

$$i\hbar\frac{\partial}{\partial t}\psi\left(\vec{r},t\right) = \left(-\frac{\hbar^2\nabla^2}{2m} + V_{\text{trap}} + U_0|\psi\left(\vec{r},t\right)|^2\right)\psi\left(\vec{r},t\right). \tag{5.1}$$

The order parameter $\psi(\vec{r},t)$ is chosen again to be some steady state background $\psi_0(\vec{r}\,)$ and a small perturbation, for the moment treated as a quantum operator, $\hat{\vartheta}(\vec{r},t)$,

$$\psi(\vec{r},t) = \left[\psi_0(\vec{r}\,) + \hat{\vartheta}(\vec{r},t)\right]e^{-i\mu t/\hbar}. \tag{5.2}$$

The presence of the quantity $e^{-i\mu t/\hbar}$ indicates the phase rotation in the overall condensate caused by the chemical potential μ, which applies not only to the steady state background but also to the perturbation. The next step is to choose the perturbation to have the form

$$\hat{\vartheta}(\vec{r},t) = \sum_i\left[\hat{u}_i(\vec{r}\,)e^{-i\omega_i t} + \hat{v}_i^*(\vec{r}\,)e^{i\omega_i t}\right], \tag{5.3}$$

where ω_i is the frequency of oscillation, and as the sum over i makes clear any perturbation can be covered by splitting it into the different components with time dependence expressible in this fashion. If this form of the order parameter is substituted into the Gross-Pitaevskii Equation 5.1, and terms evolving with the form $e^{-i\omega_i t}$ and $e^{i\omega_i t}$ are collected, the result is a pair of coupled equations in $\hat{u}_i$ and $\hat{v}_i$ for each frequency. The simple time evolution means that the time derivatives can be immediately performed, and the result are the BdG equations. Here the i subscripts have been dropped, since for the purposes of this work only single frequency solutions will be sought. The equations are

$$\begin{aligned}\hbar\omega\hat{u}(\vec{r}\,) &= \left(-\frac{\hbar^2\nabla^2}{2m} + \mathrm{V}_{\mathrm{trap}} - \mu + 2U_0|\Psi_0(\vec{r}\,)|^2\right)\hat{u}(\vec{r}\,) + U_0(\Psi_0(\vec{r}\,))^2\hat{v}(\vec{r}\,) \\ -\hbar\omega\hat{v}(\vec{r}\,) &= \left(-\frac{\hbar^2\nabla^2}{2m} + \mathrm{V}_{\mathrm{trap}} - \mu + 2U_0|\Psi_0(\vec{r}\,)|^2\right)\hat{v}(\vec{r}\,) + U_0(\Psi_0^*(\vec{r}\,))^2\hat{u}(\vec{r}\,), \quad (5.4)\end{aligned}$$

originally derived to describe the oscillations of a vortex line by Pitaevskii [35]. In this notation U_0 represents the collection of constants controlling the interaction strength between atoms, and as before

$$U_0 = \frac{4\pi\hbar^2 a}{m}, \tag{5.5}$$

with a the s-wave scattering length, which is a function of the type of atoms used in the condensate. It is these equations for which a solution indicating the presence of superradiance will be sought in Chapter 6.

Sonic Superradiance in the BdG Equations

The original analytic work aimed at deriving superradiance without the hydrodynamic equations begins from the Bogoliubov deGennes equations shown in Chapter 5, Equation 5.4. For simplicity the operator notation will be dropped in this derivation, and the perturbations u_i and v_i will be treated as functions, but there is nothing to prevent them from being treated as operators throughout. Unfortunately, the derivation will not find any solution that sheds light on the superradiance question.

6.1 Simplifying the Equations

The BdG equations can be simplified somewhat by choosing the form of the solutions that are desired, and this is necessary if any analytic solution is to be found. Starting from the equations,

$$\begin{aligned}\hbar\omega u(\vec{r}\,) &= \left(-\frac{\hbar^2\nabla^2}{2m} + \mathrm{V}_{\mathrm{trap}} - \mu + 2U_0|\Psi_0(\vec{r}\,)|^2\right) u(\vec{r}\,) + U_0(\Psi_0(\vec{r}\,))^2 v(\vec{r}\,) \\ -\hbar\omega v(\vec{r}\,) &= \left(-\frac{\hbar^2\nabla^2}{2m} + \mathrm{V}_{\mathrm{trap}} - \mu + 2U_0|\Psi_0(\vec{r}\,)|^2\right) v(\vec{r}\,) + U_0(\Psi_0^*(\vec{r}\,))^2 u(\vec{r}\,), \quad (6.1)\end{aligned}$$

the first step is to choose the coordinate system. Mirroring the derivation performed by Slatyer and Savage [11] reproduced in Chapter 4, a cylindrically symmetric system will be assumed, with no variation in the z axis. This allows the laplacian operator ∇^2 to be expanded. In addition the angular dependence of the perturbations will be chosen as $e^{iq\theta}$, so that $u = \psi_a(r)e^{iq\theta}$ and $v = \psi_b(r)e^{-iq\theta}$ a variation only of the phase. The reason for the opposite phase terms in u and v is that the actual perturbation is the sum of u and the complex conjugate of v, and it is these quantities that are expected to have the same angular dependence. Making these changes and performing the derivatives with respect to θ and z leads to this equation from the equation for u

$$\begin{aligned}\hbar\omega\psi_a(r)e^{-iq\theta} &= \left(-\frac{\hbar^2}{2m}\left[\frac{\partial^2}{\partial r^2} + \frac{1}{r}\frac{\partial}{\partial r} - \frac{q^2}{r^2}\right] - \mu + 2U_0|\Psi_0(\vec{r}\,)|^2\right)\psi_a(r)e^{iq\theta} \\ &\quad + U_0(\Psi_0(\vec{r}\,))^2\psi_b(r)e^{-iq\theta}. \qquad (6.2)\end{aligned}$$

The trap potential has been neglected here, in order to simplify the analytic derivation. This is not too drastic an approximation, and vastly increases the chances of an analytic solution. The equation for v provides an equation that is different only in the transposition of ψ_a and ψ_b, that the background term is instead the complex conjugate, and the negative frequency. In this derivation only one equation will be followed, since the process for the other is the same, and providing both would be redundant.

Further simplification can be achieved by assuming the form $\psi_a(r) = r^{-1/2}G(r), \psi_b = r^{-1/2}F(r)$, which again is a similar step to that taken in the derivation in Section 4.1. This allows a simplification of the derivatives in r, and the $r^{-1/2}$ factor can immediately be removed. In addition, the background ψ_0 will be assumed to have the form $\sqrt{n_0(r)}\, e^{il\theta}$, where $n_0(r)$ is the density distribution of the condensate, and l will be provided by the vortex charge, the number of quanta of angular momentum in the vortex forming the background. A final simplification is to remove the frequency term, by assuming that $w \to 0$. The motivation for this is to seek a situation where it is possible to decouple the equations, which is impossible with the difference between the ω terms if they are non-zero. This indicates that any solution will be a steady state one, and is made acceptable by the fact that superradiance occurs under a frequency cutoff [3]. The result of these changes is

$$0 = \left(-\frac{\hbar^2}{2m} \left[\frac{\partial^2}{\partial r^2} + \frac{1}{4r} - \frac{q^2}{r^2} \right] - \mu + 2U_0 n_0(r) \right) G(r) e^{iq\theta} + U_0 n_0(r) e^{i2l\theta} F(r) e^{-iq\theta}. \quad (6.3)$$

The angular terms provide a problematic condition on the derivation. For the solutions to be consistent all the terms in this equation have to have the same angular dependence, a condition that also applies to the mirrored equation. The conditions on the parameters are therefore

$$\begin{aligned} q &= -q + 2l, \\ -q &= q - 2l. \end{aligned} \quad (6.4)$$

Since l is fixed by the system, this therefore requires that $q = l$. This represents a much stricter requirement on the angular wavenumber of the sound wave than is expected, and it is not clear what it means. It may be a result of trying to solve a complex system analytically.

The angular requirement does allow the removal of the angular terms from the equations. In addition, the equation will be divided by the quantity $-\hbar^2/2m$, and Equation 5.5 will be substituted for U_0. This results in the equations

$$0 = \frac{\mathrm{d}^2 G}{\mathrm{d}r^2} + \frac{(1-4l^2)}{4r^2} G + \frac{2m\mu}{\hbar^2} G - 8\pi a n_0 (2G + F) \quad (6.5)$$

$$0 = \frac{\mathrm{d}^2 F}{\mathrm{d}r^2} + \frac{(1-4l^2)}{4r^2} F + \frac{2m\mu}{\hbar^2} F - 8\pi a n_0 (2F + G) \quad (6.6)$$

The equations have exactly the same terms, and so by summing them, and subtracting one from the other, two equations in two new functions can be created that are decoupled. If $Q = G - F$ then

$$0 = \frac{\mathrm{d}^2 Q}{\mathrm{d}r^2} + \frac{(1-4l^2)}{4r^2} Q + \frac{2m\mu}{\hbar^2} Q - 8\pi a n_0 Q. \quad (6.7)$$

The last element to specify is the vortex density $n_0(r)$, which to obtain an analytic solution will be defined as

$$n_0(r) = \rho_\infty \left(1 - \left(\frac{r_0}{r}\right)^2\right). \tag{6.8}$$

This density profile can really only be taken to preserve the general behaviour of a density that drops towards the centre of the system and reaches 0 at $r = r_0$, but for the purpose of finding an analytic solution it will do. The parameter r_0 represents a region of zero density, just as in the derivation in Section 4.1.

6.2 Solutions

Equation 6.7 is in fact solvable, although the solutions do not appear immediately helpful. An algebraic manipulation package gives the answer in terms of Bessel functions of the first and second kind. A Bessel function is a solution to the differential equation

$$x^2 \frac{\mathrm{d}^2 y}{\mathrm{d}x^2} + x\frac{\mathrm{d}y}{\mathrm{d}x} + (x^2 + n^2)y = 0. \tag{6.9}$$

There are two types of Bessel function, referred to as Bessel functions of the first kind $J_n(x)$ and of the second kind $Y_n(x)$, and when plotted take the form of an oscillation in positive x that diminishes in amplitude as distance from $x = 0$ increases. Bessel functions of the first kind are 0 at $x = 0$ except for $n = 0$, which has its maximum value there. Bessel functions of the second kind approach $-\infty$ as $x \to 0$. The solution given for Q is

$$Q = C_1\sqrt{r}\ J_\gamma(\kappa r) + C_2\sqrt{r}\ Y_\gamma(\kappa r) \tag{6.10}$$

where L and U are new labels given to groups of constants for the sake of clarity, with

$$\gamma = \pm\sqrt{l^2 - 8\pi a\rho_\infty r_0^2}, \quad \kappa = \sqrt{\frac{-8\pi a\rho_\infty \hbar^2 + 2m\mu}{\hbar^2}}, \tag{6.11}$$

and C_1 and C_2 are constant amplitudes. κ is restricted from being negative because the Bessel functions are undefined for negative values.

In the same way as in Section 4.1 an investigation of the asymptotic regions was attempted, in the hope that Abel's theorem can once again be used to connect the Wronskians of the solutions, since there is again no first order derivative term in the equation for Q. Conveniently, the asymptotic form of Bessel functions is well established. For $r \to 0$, the solution becomes

$$Q = \sqrt{r}\left(A\frac{1}{\Gamma(\gamma+1)}\left(\frac{\kappa r}{2}\right)^\gamma - B\frac{\Gamma(\gamma)}{\pi}\left(\frac{2}{\kappa r}\right)^\gamma\right) \tag{6.12}$$

Where $\Gamma(x)$ is the extension of the factorial to real and complex values. This solution can be rewritten as

$$Q = \sqrt{r}\left(A\frac{1}{\Gamma(\gamma+1)}e^{\gamma\ln(\kappa r/2)} - B\frac{\Gamma(\gamma)}{\pi}^{-\gamma\ln(\kappa r/2)}\right). \tag{6.13}$$

For the interpretation of the perturbation as a soundwave to make sense the solution must be oscillatory, which will be the case if γ is imaginary, which requires that $l^2 < 8\pi a\rho_\infty r_0^2$. If this is the case then the Wronskian, which as before is $W = y_1 y_2' - y_1' y_2$ can be found using the solutions with $\pm\gamma$ as the two linearly independent solutions. The result of this is that

$$W(0) = 2\gamma\left(|B|^2 - |A|^2\right) \tag{6.14}$$

The far field Wronskian is more easily derived by solving a modified form of the differential equation, since with $r \to \infty$ the $1/r^2$ term in Equation 6.7 can be neglected, which leaves a simple equation of the form

$$0 = \frac{\mathrm{d}^2 Q}{\mathrm{d}r^2} + \kappa^2 Q, \tag{6.15}$$

which can be seen to have solutions

$$Q = Ce^{i\kappa r} + De^{-i\kappa r}. \tag{6.16}$$

The Wronskian of this solution is also easy to calculate,

$$W(\infty) = 2i\kappa\left(|D|^2 - |C|^2\right) \tag{6.17}$$

As in Section 4.1 the coefficients of the waves in each asymptotic region are identified with incoming or outgoing waves, $A = 0$, $B = T$, $C = 1$, and $D = R$. Setting the Wronskians equal, which Abel's theorem requires them to be, then implies that

$$\gamma|T|^2 = i\kappa\left(|R|^2 - 1\right), \tag{6.18}$$

which then means that

$$|R|^2 = 1 + \frac{|\gamma|}{\kappa}|T|^2 \tag{6.19}$$

This implies that whenever κ is real superradiance will occur, which combined with the condition that γ is imaginary can be manipulated to give the superradiance condition

$$l^2 < 8\pi\rho_\infty a r_0^2 \tag{6.20}$$

Whether this condition can be met when expressed in this form isn't clear. However, the condition is simplified when one assumes that the radius of zero density will be of an order of roughly the healing length of the condensate ξ, as discussed elsewhere. If the radius of zero density is defined as $\epsilon\xi$ where ϵ is some number approximately equal to or less than 1 then $r_0 = \epsilon\hbar/\sqrt{2mU_0\rho_\infty}$, and $U_0 = 4\pi a\hbar^2/m$. These values inserted into the inequality together imply that for superradiance to occur it would have to be the case that $l^2 < \epsilon^2$, and since ϵ is approximately 1 or smaller, and l is the vortex charge and must be at least one, this rules out superradiance in this case.

At a number of points in the derivation very strong approximations or limitations were introduced, which means that although it would have been significant if superradiance was predicted by this solution, it is not significant that this specialised case does not produce it. Unfortunately, no more general analytic solution could be found. As such, the analytic route was abandoned, and the choice was made to numerically simulate the system, which will be discussed in the chapters that follow. The result was to some extent promising, however, since the solutions did take the form of incoming and outgoing waves both close to the vortex and far from it, which suggests that superradiance is possible in this more complete description of the behaviour of a BEC system.

Chapter 7

Preliminary Theoretical Consideration for Numeric Work

Before beginning the numerical investigation foreshadowed at the end of Chapter 6, there are a few theoretical considerations to discuss. After a brief discussion of the software to be used, a discussion follows of the choice of equations to simulate, and the selection of the equation for the background and the initial state of the perturbation, as well as the coordinate system in which to simulate.

7.1 XMDS

The first point to cover in the preliminaries to the numeric work performed is the software used in the process. In this case, use was made of a package called XMDS [31], which in basic terms is designed to convert an extensible markup language (XML) document defining a problem into a c++ program which is written with a level of optimisation that would require significant skill as a programmer to produce. In this manner it is possible for those who are not heavily versed in c++ programming to never-the-less create and run numerical simulations within the domain of XMDS which will use consistent methodology and run at a respectable speed. The problems that XMDS is designed to tackle are differential and partial differential equations. For the case of BEC superradiance the equations that are to be solved numerically will be partial differential equations, regardless of the version of the equations used, and so XMDS is ideal.

7.2 Choice of the Equations of Motion

7.2.1 The Boboliubov deGennes Equations

As in the analytic case, there are a number of possible equations that can be used to investigate fluctuations in a BEC vortex system, and it is again worth thinking about which would be most appropriate for the method being employed. Since some considerable investigation into the description provided by the Bogoliubov deGennes equations was made in Chapter 6, it might seem logical to work with that system of equations. However, such a system of equations would in fact be poorly suited to the demands of a numerical simulation, and if possible should be avoided.

The reason for this is found in the way in which the numerical simulation program that is created by XMDS performs the propagation. The most time consuming part of most simulations is propagating the system forward in time, which is unsurprising. In the case of the code generated by XMDS, the use of spatial derivatives along with time involves calculating the Fourier transform of each variable field across the entire space. On a two dimensional spatial lattice with sufficient density of points to faithfully reproduce the physics of the equations in the problem in question this Fourier transform is very time consuming. Since this is performed at each time step, it rapidly becomes the single most significant contributor to the total time taken by the simulation. Since the Bogoliubov deGennes equations are a coupled system involving two separate perturbation fields, there are two things that must be transformed at each time step. This means that although a system of equations using only one field that varies in time will not exactly halve the time taken by the simulation, it will reduce it significantly, and since a full simulation was initially expected to run for several hours at least, it is well worth seeking an alternative.

There are a number of alternative equations of motion that use one complex field to represent the perturbation, which are more attractive. The performance enhancement that such a system would provide could in principle be canceled if it were possible to remove an extra dimension from the simulation in the case of the BdG equations, but as was shown in Section 6.1, this places very strong constraints on the angular behaviour of the system, and although the analytic conclusion that in that specific case superradiance is unlikely to occur is not necessarily conclusive, given the approximations made, the constraints on the angular behaviour seem to be unhelpful if they are not required.

7.2.2 The Hydrodynamic Equations

Another form of the equations of motion that would seem a logical choice for the numerical investigation are the hydrodynamic equations derived in Section 3.3.3, although without the hydrodynamic approximation. The equations that would be used are Equations 3.37 and 3.38, which are:

$$\frac{\partial\hat{\theta}}{\partial t} = \frac{\hbar}{4m\rho_0}\nabla\cdot\left(\rho_0\nabla\left(\frac{\hat{\rho}}{\rho_0}\right)\right) - \vec{v}\cdot\nabla\hat{\theta} - \frac{U_0}{\hbar}\hat{\rho}, \tag{7.1}$$

$$\frac{\partial\hat{\rho}}{\partial t} + \frac{\hbar}{m}\nabla\cdot\left(\rho_0\nabla\hat{\theta}\right) + \nabla\cdot(\hat{\rho}\vec{v}) = 0. \tag{7.2}$$

These equations are again a coupled system with two variable fields, and converting them into a single equation with a single unknown field required the hydrodynamic approximation that this investigation is specifically avoiding. However, it could have been possible in these equations to remove the angular dependence without a constraint of the same strength on the angular dependence as occurred in the BdG case. Unfortunately, the presence of the higher derivative quantum pressure term makes coding with these equations complicated, since the input format of XMDS requires that the ∇ derivative operators be separated into individual spatial derivatives. Expanding the quantum pressure term results in a multiplicity of components of various derivative orders, which would increase the number of calculations that would need to be performed at each time step, although it would not require additional fourier transforms, it would still be less than ideal over the tens of thousands of time steps required to run a simulation. In addition, it was not clear how to go about removing the angular dependence in a self-consistent manner, so this form of the equations of motion was also discarded.

7.2.3 The Heisenberg Equation of Motion

Having come to the conclusion that neither of the simplified versions of the equation of motion for the perturbation derivation are ideal for a numerical simulation, it seems sensible to fall back on the initial equation from which both can be derived, the Heisenberg equation. As was discussed in Section 5.1, from the Heisenberg equation of motion it is possible to derive either an equation of motion for the perturbation as a mean field of the same sort as the background in the Gross-Pitaevskii equation, which is Equation 3.29, or an equation of motion that treats the perturbation as a quantum operator, as in Equation 5.2. Since aside from what they are describing these equations have the same form it is to a certain extent unnecessary to choose between them, since the numerical simulation of each would be the same.

Convenient as this is, the primary reason to prefer this form of the equation of motion for the perturbation is the simplicity of the equation. It is straightforward, and there is only one field to be calculated, albeit a complex one. This combination means that in the first instance it is simple to write the equation in the format required by XMDS, and in the second there will be no unnecessary fourier transforms performed by the code. It is also advantageous in that there has been very limited restrictions placed on the behaviour of the perturbation. In principle any initial state could be inserted into code using this equation provided it meets the condition of being small compared to the background.

For these reasons, this is the equation chosen for the numerical simulations:

$$i\hbar\frac{\partial\hat{\psi}}{\partial t} = \left(-\frac{\hbar^2\nabla^2}{2m}\right)\hat{\psi} + U_0\left(\psi_0\hat{\psi}^* + \psi_0^*\hat{\psi}\right)\psi_0 + U_0|\psi_0|^2\hat{\psi}. \tag{7.3}$$

Which is very similar to Equation 3.29, except that here, as in the analytic investigation, the decision has been made ignore the external potential of the trap, which will result in a condensate that is uniform except for the vortex. This greatly simplifies the system, and as discussed in Chapter 6 isn't an unreasonable approximation for a first investigation of this problem. The choice is also made, again for the same reasons as in the analytic discussion, to treat all the fields involved as constant along the z-axis, which means that coordinate can be ignored. The equation is here expressed in a mean field form, but it is important to remember that an operator interpretation is equally valid.

7.3 Variables and Initial State

Given that the objective of this research is to investigate superradiance in a BEC, it seems natural to use values for the various constants of the system that correspond to the real values for a BEC. For the simulations that will be described the choice of Rubidium, specifically Rb^{87}, has been made. The background vortex and initial state of the perturbation also need to be specified.

7.3.1 The Background

In the case of the vortex the density profile of the background can be generated by solving the Gross-Pitaevskii equation numerically. The result of this is a density profile that cannot be exactly matched to a function, and so although this could be used in the simulation, any simplifying coordinate transforms could require the solution to be regenerated. Instead, a function profile that is very close to the numeric solution will be used. For a charge 1 vortex such a density profile is [6]

$$\rho = \rho_\infty \frac{r}{\sqrt{2+r^2}}. \tag{7.4}$$

In this profile ρ_∞ is the density had the vortex not been present, for which a typical value for a BEC will be used, and the units in which r is measured are the healing length of the condensate far from the vortex ξ. It is important to note that this will not be the healing length near the vortex, since the healing length depends on the density and thus will change close to the vortex. In the more general case of a vortex with charge l this profile will stretch further away from the origin. In addition, the scale will be converted from the healing length to real units, in order to facilitate use of standard units throughout the simulation. As such, the density profile will be

$$\rho = \rho_\infty \frac{(r/l\xi)}{\sqrt{2+(r/l\xi)^2}} \tag{7.5}$$

The angular dependence of the vortex is more straightforward. The vortex charge again plays a role, and the requirement that the solution be single valued on a complete rotation lends itself to a complex exponential. The final background is therefore

$$\Psi_0 = \sqrt{\rho_\infty} \frac{(r/l\xi)}{\sqrt{2+(r/l\xi)^2}}\ e^{il\theta} \tag{7.6}$$

7.3.2 The Perturbation

The initial state of the perturbation used is closely modeled on the wavepacket used in the numerical simulations in the hydrodynamic approximation discussed in Section 4.2, both in order to investigate parallels between the results of the hydrodynamic approximation case and this one, and in the hope that it would provide some guidance in the parameters of the system needed to provoke superradiance. In that case the simulation was only in the radial dimension, in which the wave was gaussian. Therefore, in this two dimensional case the initial wavefunction of choice is a ring shaped wavefunction that is gaussian in the radial dimension and with only phase variation in the angular direction. In essence it is simply taking the initial state provided in Equation 4.22 and adding an angular phase variation in the form of a complex exponential with wavenumber m,

$$\psi(0,r,\theta) = e^{-(r-r_{\text{init}})^2/w^2} e^{i\omega r} e^{im\theta} \tag{7.7}$$

7.3.3 The Ergoregion

Once the choice of background and the constants in the system has been made, it is possible to predict the location of the boundary of the ergoregion. This is straightforward theoretically, but it is important, since it provides some guidance as to how the simulation is reacting, and whether it is behaving as expected. The boundary of the ergoregion is that surface in the domain where the speed of sound is equal to the magnitude of the velocity of the fluid flow. The speed of sound in a condensate is related to the local density, like so [6]

$$c_{\text{sound}} = \sqrt{\frac{4\pi\rho^2\hbar^2 a}{m_{\text{atom}}^2}} \tag{7.8}$$

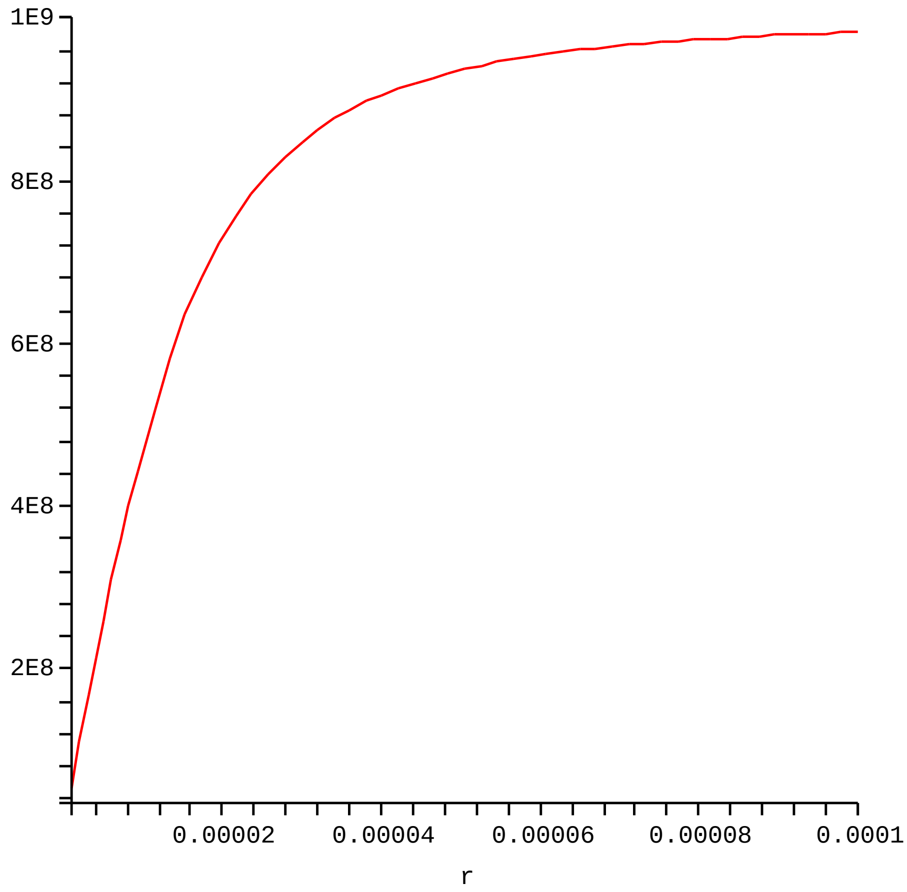

Figure 7.1: A plot of $\psi_0(r)$ of a BEC vortex as given by Equation 7.6. The charge of the vortex in this case is 5, and constants corresponding to Rb^{87} have been used to generate it. The unperturbed density ρ_∞ was set to 1×10^{18}. For reference, the healing length far from the vortex in the system is about 2.6×10^{-6}, so the range of r here is about 40 healing lengths, in contrast to the 5 healing length radius of a vortex with charge 1.

The result of this is that the speed of sound follows the density down as the center of the vortex is approached. This can be more clearly illustrated by means of plots, so they are provided. Figure 7.1 is a plot of the variation in r of ψ_0 as given by Equation 7.6 with typical constant values. Figure 7.2 is a plot of the speed of sound as calculated from that density profile and Equation 7.8. The characteristics of the drop in the speed of sound can thus be observed in comparison with the drop in density.

In contrast with the speed of sound in the vortex, the speed of flow in the BEC increases as the center of the condensate is reached. The quantisation of angular momentum found in the BEC means there is a direct link between the vortex charge and the speed of rotation. The speed is given by

$$v_\theta = \frac{\hbar l}{m_{\text{atom}} r} \tag{7.9}$$

This is of course a hyperbolic plot, which can be expected to grow sharply at some point

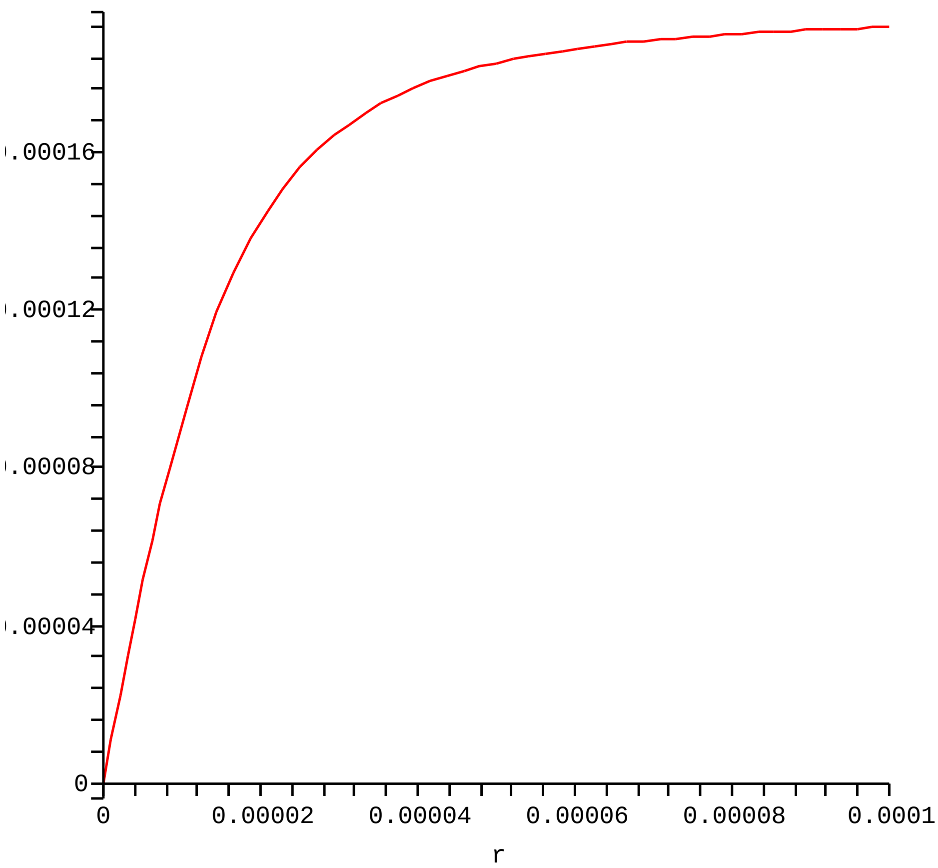

Figure 7.2: A plot of the speed of sound in a BEC vortex as calculated from the density profile in Figure 7.1 and Equation 7.8. The vortex charge is 5, and the use of standard units throughout indicates that the speed is measured in m/s.

in the r domain. The ergoregion boundary, or ergosphere, will be found at the intersection between this function and Equation 7.8. Although the resulting equality leads to an equation that appears complicated due to the large number of constants involved, the only actually variable elements are the density and the $1/r$ dependence in the speed of flow, and the equation can be solved straightforwardly, to give two real and two complex possible values for r. Clearly, the two complex values are inappropriate answers, and of the two real solutions one is negative, so there is only one physically appropriate solution choice. The ergoregion boundary will be found at

$$r = \sqrt{\frac{1+\sqrt{5}}{8\pi a \rho_\infty}} l, \tag{7.10}$$

and since the healing length of the condensate far from the vortex ξ is given by $1/\sqrt{8\pi a \rho_\infty}$, the ergoregion boundary is at

$$r = \sqrt{1+\sqrt{5}} \cdot \xi l. \tag{7.11}$$

$\sqrt{1+\sqrt{5}}$ is about 1.8, to provide a direct numeric idea of the scale. Remember that for a charge 1 vortex the radius of the density perturbation is about 5 healing lengths, and this expression states that the ergoregion boundary for such a vortex will have a radius of about 1.8 healing lengths.

7.3.4 Coordinate System

Although initially both the background and the perturbation have angular dependencies that exist only in the phase, there is no firm guarantee that this will continue to be the case. This means that although initially cylindrical polar coordinates would seem the logical choice of coordinate system to work in, there is some value in starting in rectangular coordinates, which will also provide the benefit of a simpler form of the laplacian operator ∇^2. It is also advantageous in that the fourier transform libraries used by XMDS require periodic boundary conditions in all the spatial variables involved. This would require an extension into $-r$ of the problem when used cylindrical coordinates. Since it is unknown whether the sound wave in the condensate will reach the centre of the system, this could in principle lead to unexpected effects as the wave and the negative extension of the wave cross at the origin. It is also the case that the negative extension results in a duplication of computational effort, wasting almost half of the calculations performed. Cartesian coordinates are therefore the starting point for the numerical work described in the next chapter, although more will be said on the issue there.

7.4 Criteria for Correct Behaviour

If a simulation produces results, it is important to have some criteria by which those results can be judged to be accurate. The typical way in which this is done is to generate simulations of situations that have analytically derivable or well known results, so the data produced by the simulation can be compared to these known values, thereby verifying that in these cases the right answers are being given. Another possibility is to have the simulation generate values throughout the run that allow an inspection of how certain parameters the correct behaviour of which is known are evolving. In the fashion, it is again possible to judge the accuracy of the simulation. In the ideal case both methods can be employed, and this is the case here.

An ideal analytically familiar case is to propagate the same initial state through a uniform condensate. In this case the wave will simply travel towards the centre of the condensate, with the gaussian shape guaranteeing a simple evolution of the shape of the wave. As for parameters that can be inspected throughout the simulation, there are a couple that can be used. The first is the number of particles in the perturbation. If superradiance actually occurs then the amplitude of the wave should grow, and presumably so would the number, but this will only happen during the interaction with the vortex. Before and after this happens one would expect the number to remain constant. In the program this will equate to a sum of the amplitudes at every spatial lattice point.

The other check on the behaviour of the wave is the momentum. This can be tracked through the fourier transform of the wave, which initially would be expected to also take the shape of a gaussian ring, given the initial state provided, and again would be expected to change only when the interaction with the vortex is taking place. Taking samples of this value and the number throughout the interval of the simulation provides some idea as to the accuracy of the simulation.

Chapter 8

Numeric Results

8.1 Initial Problems

Creating an XML script that can be compiled by XMDS to simulate the BEC perturbation system in rectangular coordinates by itself is not especially difficult. Creating a script with as little as possible calculated on each iteration of the propagation likewise is not especially significant. That said, even in this relatively simple situation errors are inevitable, and not always easy to track down. As such, when the simulation that was written initially did not appear to reproduce the expected behaviour, the natural reaction was to seek out and remedy those bugs.

Once the initial state was generated correctly, the momentum was as expected, the number of particles in the perturbation was conserved approaching the vortex, and the gaussian wave was traveling as expected in the region of the domain where the condensate density was unperturbed, it appeared that everything in the code was working as expected. A picture of the density of the perturbation initial state is provided in Figure 8.1, and the real part of the initial state is Figure 8.1. A closer picture of the way the angular variation changes is seen in Figure 8.1, where the combined angular and radial variation result in an interlacing of the angular peaks, and a cross section of the wave showing a picture of how it varies in the radial direction is shown in Figure 8.1. A sample of the background density makes the drop off of the vortex clear, as can be seen in Figure 8.1, and the shape is more clearly visible on a slice close to the x-axis, Figure 8.1. The reason for the slice being close to but not along the x-axis is that the presence of behaviour depending on $1/r$ in the problem means the presence of a lattice point at 0 on either axis could lead to errors.

When this was all working, the previous short time domains over which the simulation ran were extended, and the perturbation was propagated all the way to the vortex, and in principle, all the way back again. Unfortunately, when this was done the wave did not reflect from the vortex as expected. Instead, the entirety of the perturbation slowly gathered into the centre of the vortex, and remained there seemingly indefinitely.

Lacking any obvious errors in the equations in the code, or any other part of the script, there are two obvious places to look for problems. The first is in the lattice being used by the simulation. A numerical simulation obviously cannot calculate the field being solved numerically with an infinite number of points, as would be the result of an analytic calculation. This would require an astonishing amount of calculations, and consequently an unreasonable amount of computing resources. As a consequence, the normal method in numerical studies is to select a number of points through the space and calculate the fields at those locations. These "lattice points" are normally evenly spaced throughout the spatial domain. In addition to this, a similar procedure is applied in the time domain,

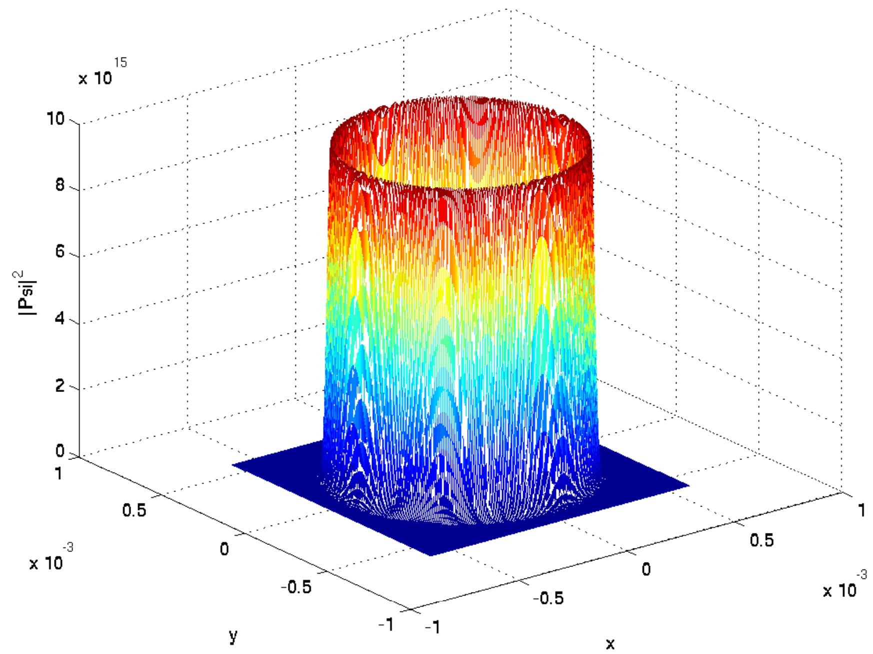

Figure 8.1: Density of the initial state in the numeric simulations.

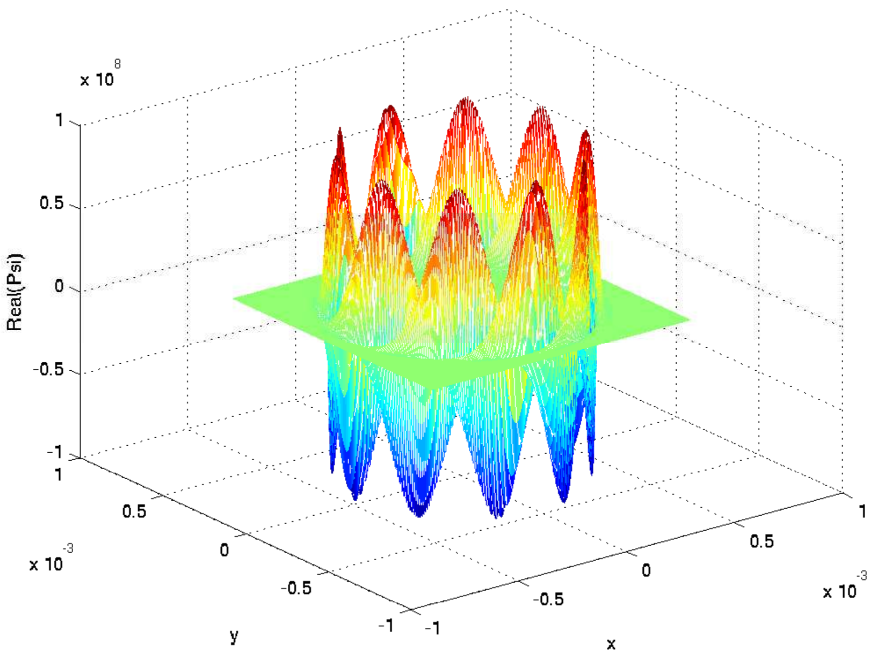

Figure 8.2: Real part of the initial state of the numeric perturbation.

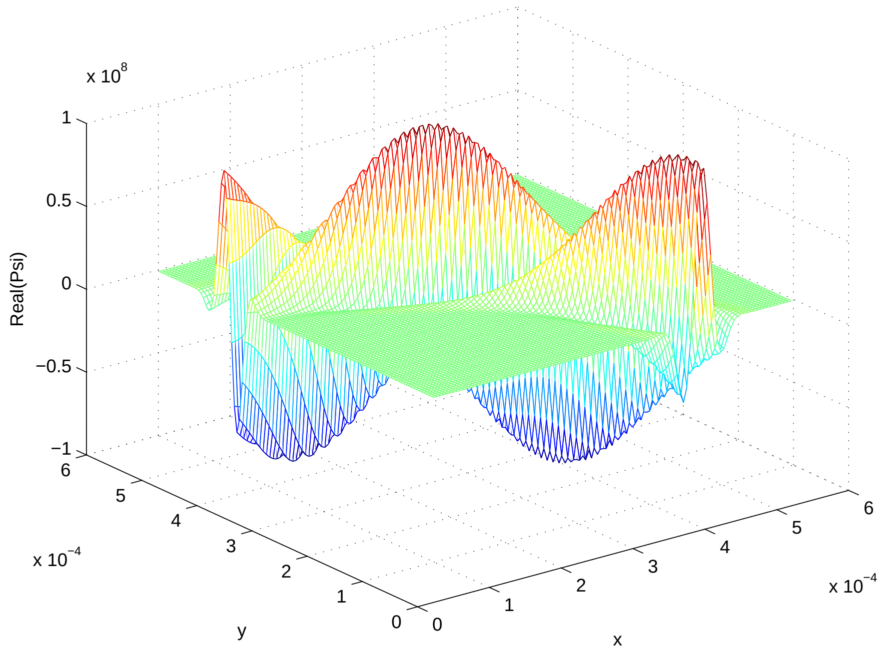

Figure 8.3: Enlargement of the 1st quadrant of the real part of the initial state.

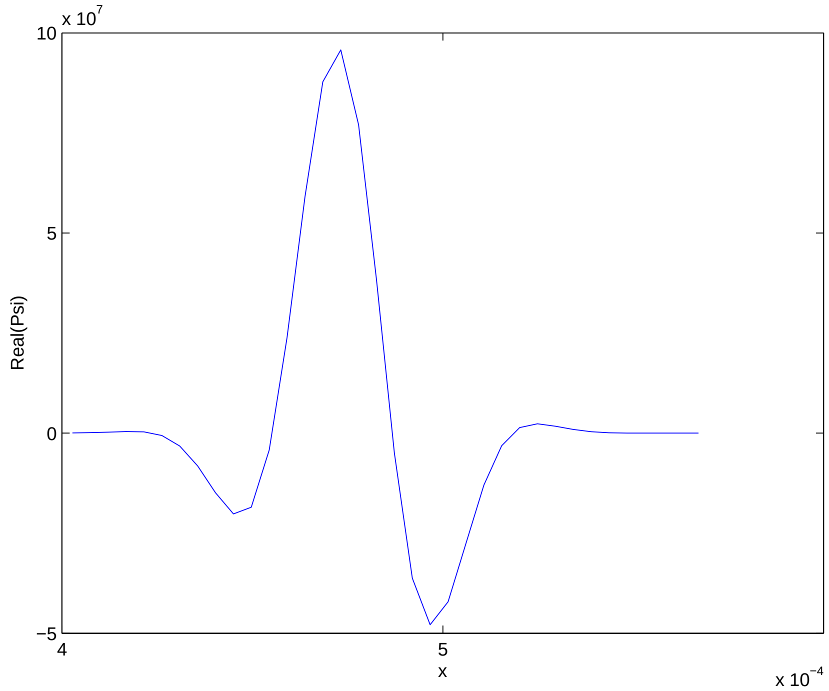

Figure 8.4: Plot of the variation of the real part of the initial state in the radial direction.

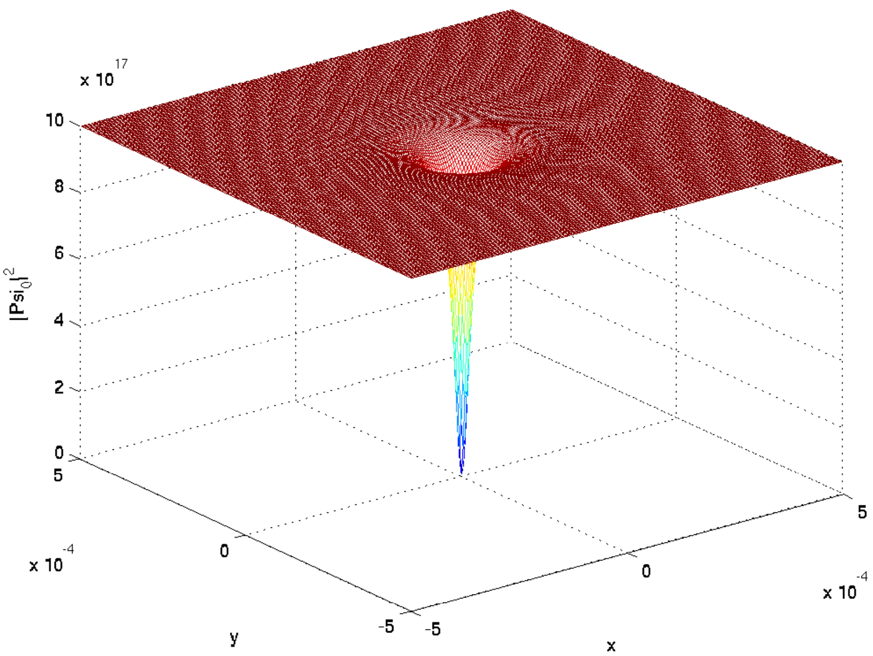

Figure 8.5: Plot of the background density of the condensate showing the density variation from a charge 5 vortex.

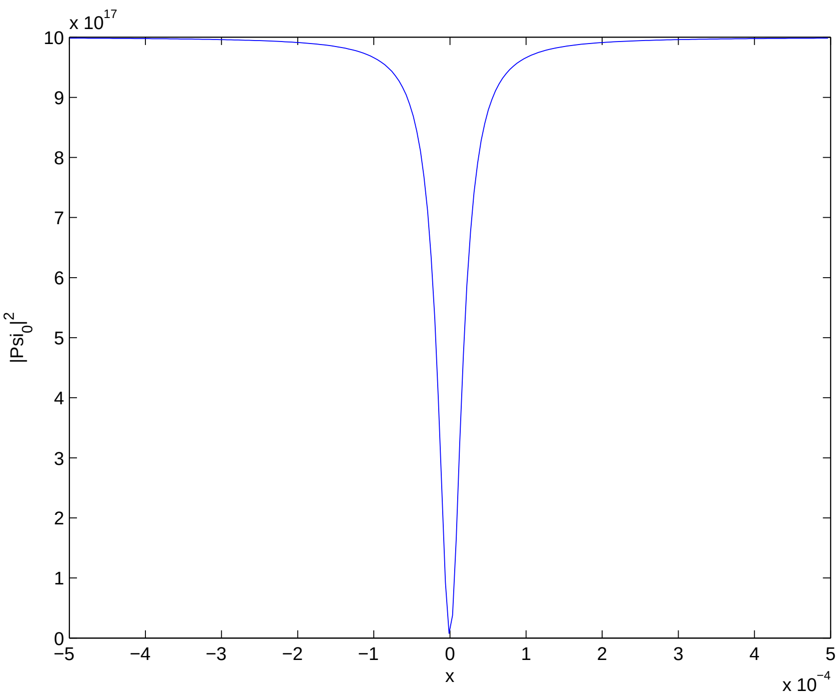

Figure 8.6: Plot of the background density on a slice close to the x-axis.

with the propagation calculated after a time step set by the code. This discretisation of the time and space domains can introduce errors into the calculations, so this needs to be corrected.

XMDS has in recent versions introduced an algorithm referred to as an adaptive time step algorithm. This selects the time step appropriate to the problem at each iteration, thereby overcoming the problem of setting the time step. It does this by calculating the result of the equations of motion with one time step, and then calculating again with a time step of half the previous one. The code compares these two values, and if there is a difference in a peak with a value greater than some percentage of the peak value, and with the magnitude of the difference greater than some cut off, then the algorithm rejects that calculation and starts again with the smaller time step. In this way, the code reaches a time step that minimises the discretisation error while also being the longest acceptable. This is a good compromise between the needs for long time steps to speed the simulation and short time steps to reduce the error. In the case of these simulations the error threshold and the value of perturbation where errors would be sought were sufficient to ensure that the time step was not the cause of the error, which was further ensured when tightening these criteria did not produce a change.

In the spatial variables the first criterion for whether the gap between lattice points is small enough is found in the variation of the fields involved. If the variation is too rapid compared to the lattice spacing errors are inevitable. In this case, the two important variations to keep an eye on are the variation in r, where the perturbation is a wave within a gaussian envelope, and the variation in θ, where there is an oscillation all the way around the ring. The rate of variation in both cases is much slower than the gaps in the lattice spacing, so that is not a problem. The final region where spatial discretisation error might creep in is the vortex itself. With the tighter confines and lower densities within this region it is possible that a higher lattice point density is necessary to correctly model the behaviour of the perturbation. If this is the case the gains in lattice density there possible through the straightforward method of increasing the number of lattice points used overall was not sufficient to fix the problem before the size of the lattice made the time taken for the full time domain to be covered unreasonable. An alternative to simply increasing the number of lattice points is discussed in Section 8.2.1.

The second possible area for problems is in the parameters describing the sound wave, specifically the angular wavenumber and radial frequency, which are effectively free parameters of the simulation, and the charge of the vortex. The charge of the vortex used initially was 1, since that was the form most expected in a genuine experimental situation. This of course implies that the ergoregion boundary is close to the centre of the vortex, which could have led to too few lattice points within the ergoregion within which superradiance could occur. Attempts to move this further out by increasing the vortex charge were unsuccessful, but the choice was made to remain at 5 for the larger ergoregion, in case it became an issue later. The radial frequency is an area of particular suspicion, since the astrophysical superradiance effect indicates that a low frequency is necessary for the effect to occur. This is counterbalanced by the requirement for a high frequency in order for the wave to have an entire wavelength within a reasonable distance given the scale of the system, which exists over a length of about a millimeter in each direction. Variation of the frequency by orders of magnitude were not, however, sufficient to resolve the problem, since very little variation in behaviour occurred. The final parameter that could be expected to change things was the angular wavenumber of the perturbation. The condition for superradiance derived in the hydrodynamic approximation work, Equation

4.21, suggests that the angular wavenumber should be high, which is counterbalanced by the consideration that it needs to be low enough for the variation to occur over a longer length scale than the lattice separation. Again, significant variation in this parameter did not produce appreciable variation in the behaviour of the wave.

8.2 Responses to the Lack of Reflection

8.2.1 Coordinate Transformation

Given the lack of effect that varying the parameters was having, the conclusion was that it likely was the density of lattice points in the vortex and especially the ergoregion that was leading to the lack of reflection. As mentioned previously, it after increasing the number of lattice points up to the practical maximum there was no change in result, so an alternative was needed.

In order to increase the number of lattice points in the vortex region without increasing the overall number of points a coordinate transformation was sought. The code for the numeric simulation chooses the lattice spacing by picking points separated equally along the range in a spatial variable. In order to concentrate more points in a given area in real space what is required is a transformation such that the region of real space of interest is changed at a different rate than the rest of the domain. There are a number of nonlinear transforms that can create this sort of situation, ranging from simple transformations like $x' = tan(x)$ to sophisticated constructions with multiple free parameters.

Given the cylindrical shape of the vortex, the transformation of most use will effect a radial coordinate. However, the use of rectangular coordinates in the simulation up until this point will complicate doing so excessively. In order to correctly define the initial state a transformation that is simple both ways is desired, and a transformation of this type was found.

Unfortunately, because of the need to work in rectangular coordinates it became necessary to apply the transformation to cartesian coordinates. As a result what had been a somewhat straightforward conversion of a single variable into a transformed version became a complicated entanglement of two variables converted into two more, an inevitable consequence of trying to work in rectangular coordinates when studying a polar problem. In particular, the laplacian in transformed coordinates involved coefficients with in excess of 80 terms, which were concluded to be impractical. Errors in the coefficients as entered into the code would be hard to catch, and if the algebraic manipulation software used to derive them was in error a check by hand could easily fail to catch it.

8.2.2 Radial Coordinates

Of course, the transformation that is difficult to make work in rectangular coordinates would work fine in cylindrical polar coordinates, since it represents a transformation in only one of the coordinates. In addition, although half of the lattice in the r dimension would be essentially wasted, it is possible using cylindrical coordinates to use a much smaller number of lattice points in the angular coordinate θ, since the variation in that direction is much slower. As a consequence the obvious step was to try a simulation in those coordinates. It was discussed in Section 7.3.4 why this is note necessarily an ideal choice for the simulation, but given the problems that were experienced it was worth a shot. The extension of the background and initial state were selected as symmetric, and a conversion to the transformation such that it worked either side of the origin were accomplished, the laplacian in the transformed coordinates was calculated, and the script was tested.

Unfortunately, a problem became immediately apparent. On the lattice points either side of zero in r' the perturbation was growing a strong density spike very quickly, beginning almost immediately after the simulation began. The spike would rapidly grow to the point at which it represented an error strong enough for the adaptive time step algorithm to notice it, at which point the time step dropped sharply and the rate of growth of the spike would slow to crawl. Unfortunately, the drop in time step was from approximately 1×10^{-6} seconds per time step to 1×10^{-10} seconds. At the larger time step full simulations at the necessary lattice sizes took hours, and this would cause a ten thousand fold increase in that duration. Changing the tolerance of the adaptive time step so it began to account for this central spike earlier did slightly increase the time step that could be taken, but not enough to be practical given the need for multiple runs of the simulation to solve the problem, and in addition to this the spike was still growing.

Various attempts to fix the problem were made. It became clear that using an untransformed radial coordinate reduced the magnitude of the problem somewhat, but increasing the number of lattice points on that coordinate increased the rate of growth of the central spike again. It was also discovered that a drastic reduction in the lattice for the angular coordinate, which was made possible by the delta function character of the fourier transform of the angular variation, unsurprising since the initial state was a perfect ring. In fact, it became apparent that by reducing the system into a pair of modes the angular variable could be eliminated, because the initial choices of angular dependence were complex exponentials, and thus eigenstates of the system. The modes needed were the mode in which the wavefunction began, and the mode into which the vortex would couple it. Unfortunately, this was still insufficient to solve the problem posed by the spike, although expressed in this way the spike no longer grew once the time step had dropped to the value around 1×10^{-10} seconds.

After an extended period of time was spent searching in vain for the cause of the problem, or some way to speed up the simulation, it was eventually concluded that there was no apparent way around the problem, and that further time spent on the problem would be wasted at present, since no further promising avenues of exploration were apparent. As such, the cylindrical coordinates were abandoned.

8.3 A New Problem

One thing that had been thrown up in the search for what was causing the spike in cylindrical coordinates was that the background had not been correctly defined. Although the correct background to use is that in Equation 7.6, what had in fact been used previously was scaled differently, and in particular did not include the scaling as a consequence of the vortex charge. This had not provided a solution when attempting to fix the problem of the central spike in the cylindrical coordinate simulation, so it was decided to turn again to rectangular coordinates with this error fixed. Unfortunately, the new script suffered from a very drastic new problem. In previous simulations the number had, as expected, remained constant until the vortex, although the fact that it remained constant during the interaction with the vortex was not as expected. Now, however, the number changed dramatically over the interval, as can be seen in Figure 8.3, which shows the fluctuation in number over half a second. This fluctuation in the number was coupled with major

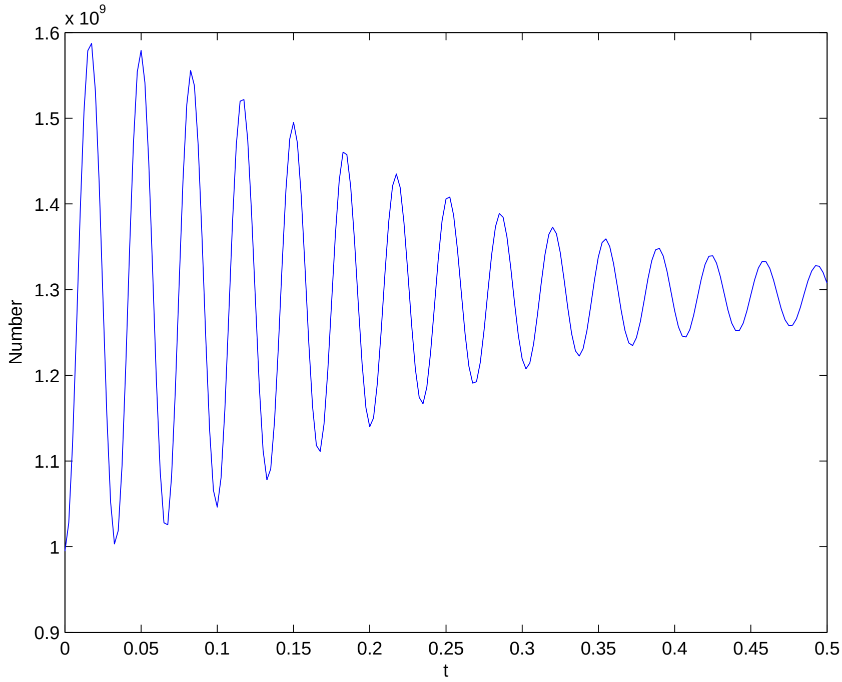

Figure 8.7: Plot of the number generated by the new cartesian script. Note that although the variation appears to be dying off towards the right of the plot it in fact becomes larger again when the simulation is continued.

changes to the density as time went on, with Figure 8.3 showing the perturbation less than a ten thousandth of a second after the simulation began, where a full simulation would run for around 5 seconds.

Clearly this was an error, and as before an attempt was made to identify what had caused it. A period of testing appeared to exonerate any of the optimisation changes made since the previous cartesian simulation, and it appeared to be the change to the correct background that had brought about the error. The introduction of the ring of radial variation into the perturbation wave function almost immediately suggested that the cause was the term in the equation of motion that included the background squared, since that was a term that retained radial variation. This term

$$U_0\psi_0^2\hat{\psi}^* \tag{8.1}$$

when removed form the equation of motion fixed the drastic number variation, resulting in a wave that could be propagated all the way to the vortex, the result of which is shown in Figure 8.3. Once again, there is no reflection, but the behaviour is similar to that found when the simulation was previously run in cartesian coordinates. With the term in Equation 8.1 included the behaviour rapidly becomes so erratic that continued propagation with any expectation of accuracy is impossible. Why this problem should suddenly occur is not clear. The only solutions that come to mind is that perhaps without the correct scaling the background term was not of the same scale as the other terms in the equation, and therefore was not able to produce this type of behaviour, or that there

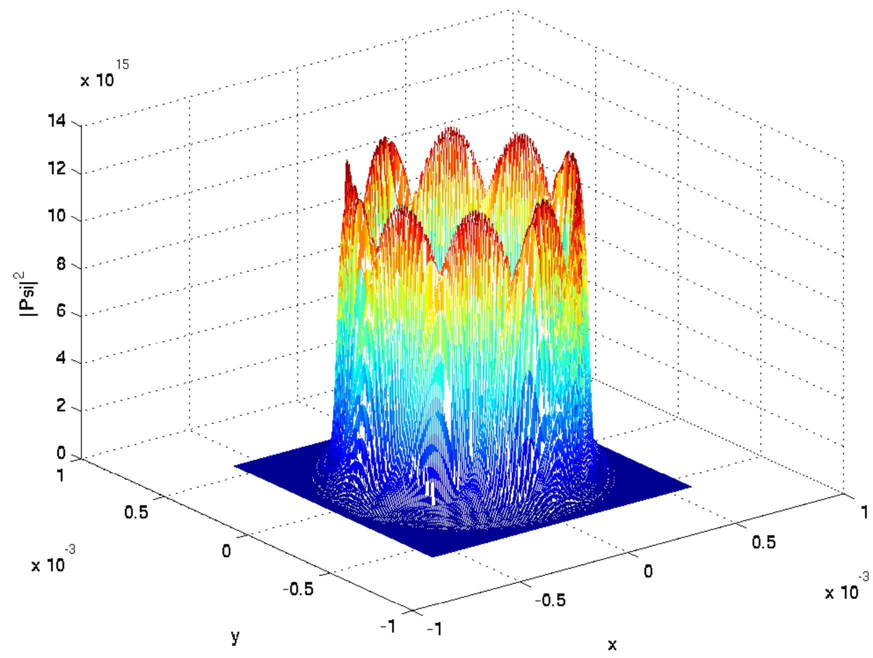

Figure 8.8: Plot of the density of the perturbation shortly after the beginning of the simulation. A marked contrast to the initial state shown in Figure 8.1.

is in fact an error in the script that was not clear.

Unfortunately it was at this point that the time at which it is no longer reasonable to continue research in an honours year had been reached. How to resolve the problem in the code was not clear, as variations in lattice points and free parameters had not produced any marked effect in the degree of the problem, although the shape had been changed by doing so. With insufficient time left to investigate and address the problem it is here that the matter must be laid to rest, which is regrettable.

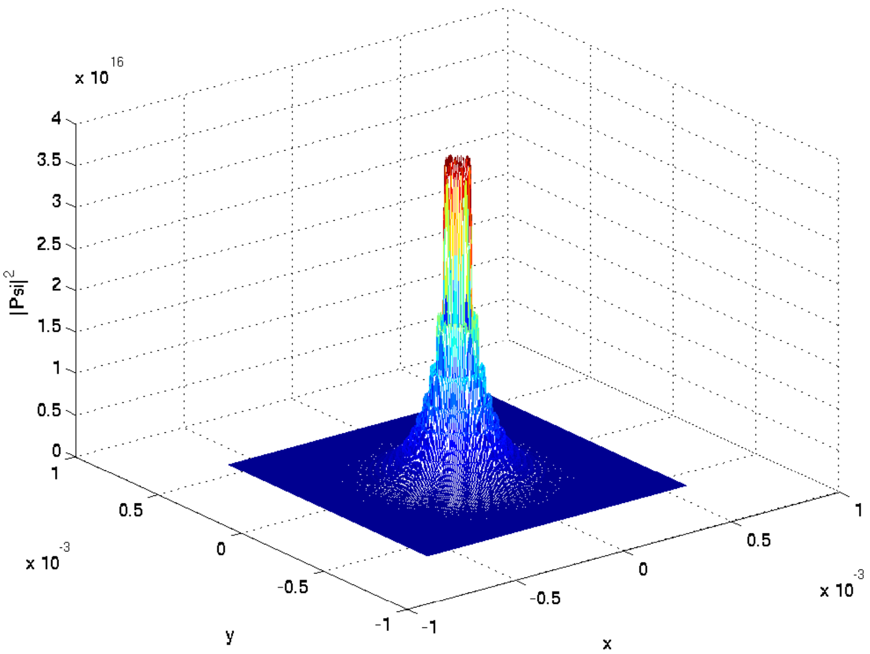

Figure 8.9: A plot of the final state reached by the numeric simulation in cartesian coordinates when the term shown in Equation 8.1 is removed.

Chapter 9

Conclusions and Future Directions

9.1 Conclusions

It is clear from the literature that the analogy between gravitational systems and fluid flows is mathematically sound, and also of great interest in the investigation of certain phenomena predicted by calculations in general relativity, Hawking radiation and superradiance among them. Bose-Einstein Condensates are interesting as systems in which to search for analogies because they have a well understood quantum description, which therefore allows the investigation of phenomena like Hawking radiation, that depend crucially on the quantum behaviour of the system. In addition, in a BEC it is easier to control the flow of the condensate than in other zero viscosity systems.

These advantages mean that investigation of Hawking radiation in BECs is interesting. However, it is also the case that Hawking radiation is a very small effect, and therefore it is advantageous to first seek to understand and observe a more pronounced phenomena in a BEC, such as superradiance. In addition to this, investigation of superradiance is interesting in its own right, and the control that is possible with a BEC makes them a promising system for that purpose, despite the fact that the quantum underpinning that a BEC provides to Hawking radiation is not required for superradiance.

The desire to perform experiments to observe superradiance provides a need for a theoretical analysis of whether superradiance can in fact be expected to occur in a BEC. There has been some analysis of this question, particularly by Slatyer and Savage [11], but all of this has relied on the dubious hydrodynamic approximation, which ignores a higher derivative term in the equations describing a condensate. This term has an order proportional to the rate of change of the density in the condensate, and in the case of a vortex in a BEC the rate of density change towards the core of the vortex is too high for this approximation to be trusted. It is also the case that it is in precisely this region where the process that gives rise to superradiance occurs. As such there is a need for an investigation of superradiance that does not make the hydrodynamic approximation, which was the focus of the original work related here.

Initial attempts to find an analytic solution to the system without the hydrodynamic approximation using the Bogoliubov deGennes equations failed due to the inability to find a solution general enough to predict superradiance. Instead a very restricted solution which predicted that superradiance would not occur in the very narrow circumstances within which the solution was valid was all that could be arrived at analytically. The behaviour of the solutions did however suggest that the possibility of an incident wave splitting into a transmitted and a reflected wave was feasible.

As a consequence of the failure to find an analytic solution of use in the system, a numerical solution for a wavepacket incident on the vortex was sought. After consideration of the theoretical background for such a simulation the XMDS package [31] was used to solve the system. Unfortunately it was not possible in the time available to solve the problems in the script. At first the sound wave was not reflected from the vortex ergoregion as expected, and the final version of the code is also plagued by a failure to preserve the number of the wave as it travels toward the vortex, in contrast with analytic predictions. Inadequate time meant that it was not possible to determine whether this behaviour was a flaw in the numerical method itself or an error in the script as written, although it was clear that if an error is responsible it is not an obvious one.

This means that the primary question, does superradiance occur in a BEC, has not yet been answered. The analytic investigation looking for a steady state solution were promising but inconclusive, and the flaws in the numerical simulation could not be located and fixed in the time available.

9.2 Future Directions

The failure to resolve the question on which the research here presented was focused indicates that there is still a great deal of work to be done on the question. The numerical script used to simulate the system seems to have some flaws hidden within it. As a result, more time and effort could be spent on seeking out and remedying those flaws. It is also of note that the numerical methods used are those commonly employed by theoreticians in the field of Bose Einstein Condensation. It is possible that an investigation of the methods used to simulate gravitational systems by cosmologists would provide an alternative way to proceed with the numerics that could perhaps be more fruitful. It also cannot be ruled out that investigation using a different form of the equations of motion could more easily yield numeric or even analytic results, and perhaps investigation in those formulations of the equations rejected in this work would be worth considering when the time taken by simulations using those equations is not so great a constraint.

There are a number of other theoretical questions related to the question of existence of sonic superradiance that also need to be answered before an experiment can be performed. It is at present not clear how any perturbation of a condensate could be measured in an ongoing fashion, since present detection methods involve the destruction of the condensate (references?). It is also not clear how the initial perturbation can be generated with the control necessary to duplicate experimental parameters like the frequency and angular wavenumber reliably. Answers to both of these questions would be as essential to an experimental investigation of superradiance in BECs as a demonstration that the effect can be expected to occur. In addition, further research in these directions has the advantage of being essential to several other research questions in the field.

Another possible direction for further research is to turn directly to Hawking radiation and investigate whether it will occur in a BEC, without taking the intermediate step through superradiance that partially motivated this research, a course that has been taken in some research already.

Bibliography

[1] B. F. Schutz, *A First Course in General Relativity*, Cambridge University Press, 1985.

[2] S. W. Hawking, Nature **248**, 30 (1974).

[3] S. W. Hawking, Commun. Math. Phys. **43**, 199 (1975).

[4] A. Vilenkin, Physics Letters **78B**, 301 (1978).

[5] W. G. Unruh, Phys. Rev. Lett. **46**, 1351 (1981).

[6] C. Pethick and H. Smith, *Bose-Einstein Condensation in Dilute Gases*, Cambridge University Press, 2002.

[7] L. Pitaevskii and S. Stringari, *Bose-Einstein Condensation*, Oxford University Press, 2003.

[8] M. Anderson et al., Science **269**, 198 (1995).

[9] C. Bradley et al., Phys. Rev. Lett. **75**, 1687 (1995).

[10] K. Davis et al., Phys. Rev. Lett. **75**, 3969 (1995).

[11] T. Slatyer and C. M. Savage, Class. Quant. Grav. **22**, 3833 (2005).

[12] M. Visser, *Artificial Black Holes*, World Scientific, 2002.

[13] M. Visser, Class. Quant. Grav. **15**, 1767 (1998).

[14] T. Jacobson, Phys. Rev. D **44**, 1731 (1991).

[15] W. G. Unruh, Phys. Rev. D **51**, 2827 (1995).

[16] S. Corley, Phys. Rev. D **57**, 6280 (1998).

[17] R. Parentani, Inte. J. Mod. Phys. **A17**, 2721 (2002).

[18] R. Schutzhold and W. G. Unruh, Phys. Rev. D **66**, 044019 (2002).

[19] R.Schutzhold and W. G. Unruh, Phys. Rev. D **68**, 024008 (2003).

[20] C. Barceló, S. Liberati, and M. Visser, Phys. Rev. A **68**, 053613 (2003).

[21] S. Basak and P. Majunder, Class. Quant. Grav. **20**, 2929 (2003).

[22] G. E. Volovik, J. Low Temp. Phys. **24**, 127 (1998).

[23] T. Vachaspati, arxiv:cond-mat/0404480, 2004.

[24] C. Barceló, S. Liberati, and M. Visser, Class. Quant. Grav. **18**, 1137 (2001).

[25] G. E. Volovik, JETP Lett. **69**, 705 (1999).

[26] G. E. Volovik, Physics Reports **351**, 195 (2001).

[27] S. Bose, Z. Phys. **26**, 178 (1924).

[28] A. Einstein, Preussische Akad. Wissenschaften **3**, 261 (1924).

[29] T. P. Simula, S. M. M. Virtanen, and M. M. Salomaa, Phys. Rev. A **65**, 033614 (2002).

[30] A. A. Svidzinsky and A. L. Fetter, Phys. Rev. A **58**, 3168 (1998).

[31] The xmds package and documentation can be found at http://www.xmds.org.

[32] U. Leonhardt, T. Kiss, and P. Öhberg, J. Opt. B:Quantum Semiclass. Opt. **5**, S42 (2003).

[33] D. L. Fetter, A. A. Svidzinsky, A. L. Fetter, and C. W. CLark, Phys. Rev. Lett. **86**, 564 (2001).

[34] M. V. Carlos Barceló, Stefano Liberati, Analouge gravity, arxiv:gr-qc/0505065, 2005.

[35] L. P. Pitaevskii, Zh. Eksp. Teor. Fys. **40**, 646 (1961).